Article

Pd-Au-Y as Efficient Catalyst for C-C Coupling Reactions, Benzylic C-H Bond Activation and Oxidation of Ethanol for Synthesis of Cinnamaldehydes

Mukesh Sharma, Biraj Das, Manash J Baruah, Subir Biswas, Subhasish Roy, Anil Hazarika, Suresh K. Bhargava, and Kusum K. Bania

ACS Catal., **Just Accepted Manuscript** • Publication Date (Web): 22 May 2019

Pd-Au-Y as Efficient Catalyst for C-C Coupling Reactions, Benzylic C-H Bond Activation and Oxidation of Ethanol for Synthesis of Cinnamaldehydes

Mukesh Sharma,[a] Biraj Das,[a] Manash J. Baruah,[a] Subir Biswas,[a] Subhasish Roy,[b] Anil Hazarika,[c] Suresh K. Bhargava[d] and Kusum K. Bania[a,d]*

[a]*Department of Chemical Sciences, Tezpur University, Assam, India, 784028*
[b]*Department of Chemistry, Indian Institute of Technology, Guwahati, India, 781039*
[c]*Department of Electronics and Communication Engineering, Tezpur University, Assam India, 784028*
[d]*Centre for Advanced Materials and Industrial Chemistry (CAMIC), School of Science, RMIT University, G.P.O. Box 2476, Melbourne 3001, Australia*

ABSTRACT:

Pd-Au nanoalloy supported on zeolite-Y (Pd-Au-Y) matrix was found to be an effective catalyst for C-Cl bond activation and oxidative coupling of 2-naphthol leading to the formation of various biaryl products and 1,1′-bi-2-naphthol, BINOL. The same catalyst was also highly efficient for selective oxidation of benzylic alcohols to benzaldehydes. Cinnamaldehydes were obtained directly from benzaldehydes by aldol condensation with acetaldehyde generated *in situ* by partial oxidation of ethanol in presence of Pd-Au-Y catalyst at 120 ^{o}C under basic condition. The biaryl products were also obtained directly from benzylic alcohols in a one-pot system by reacting with phenylboronic acid. The formation of biaryls from benzylic alcohols was believed to occur *via* one-pot benzylic C-H and C-Cl bond activation. A high % yield of biaryls, BINOL, aldehydes and cinnamaldehydes were obtained by performing different reactions using the single Pd-Au-Y catalyst. The strong interaction of chloro-benzylic alcohol was predominantly located at active gold species. X-ray photoelectron and diffuse reflectance spectroscopic studies revealed for the strong interaction between Pd and Au particles. Electrochemical studies provided a proper evidence for the individual role of the nanoparticles (NPs) in one-pot synthesis of biaryls from benzylic alcohols.

Keywords: Pd-Au NPs, Zeolite-Y, Biaryls, Aldehydes, BINOL, Cinnamaldehydes

1. INTRODUCTION

C-Cl bond activation, oxidative coupling of 2-naphthols, selective oxidation of alcohols and aldol-type condensation reaction leading to the formation of C-C coupled product, aldehyde and cinnamaldehyde are considered to be some of the important classes of organic reactions.[1-14] Out of the different form of Suzuki-Miyaura cross-coupling (SMCC) reactions, the formation of biaryls by C-Cl bond activation is highly appreciable due to the low cost of chloro-derivatives compounds.[7,8,15-19] Pd-based catalysts either in the homogeneous or heterogeneous form are best known for SMCC reaction.[5,8,20-22] However, it has been found that the C-Cl bond activation process with single Pd metal is less effective.[5,7,8] Recent studies suggested that alloying of Pd with other metals like Ni, Au, Co etc. led to successful activation of C-Cl bond in SMCC reaction.[5,7,8,23] We also found that Pd-NiO nanocatalyst supported on the zeolite-Y matrix to be an effective heterogeneous catalyst for C-Cl bond activation in SMCC reaction.[7] As the reports on C-Cl bond activation for biaryl product formation is limited, therefore finding a highly active and reusable heterogeneous catalyst for C-Cl bond activation would be highly beneficial.

Apart from the coupling of aryl chlorides, the oxidative coupling of 2-naphthol to 1,1′-bi-2-naphthol commonly known as BINOL is considered to be an important oxidative coupling reaction due to the high applicability of BINOL in pharmaceutical product and also as chiral auxiliary.[9-11,24] The oxidative coupling of 2-naphthol is rather a difficult process as the yield is often very poor. Fe (III)-Schiff base catalysts are better known for such catalytic conversion.[10,11,24] Most of the catalytic oxidation of 2-naphthol to BINOL are performed using air or molecular oxygen (O_2).[9-11,24] O_2 as oxidant is considered to be the most preferential approach.[25-27] The oxidation process with hydrogen peroxide (H_2O_2) as oxidant is restricted by the formation of several other byproducts reducing the BINOL formation or its

selectivity.[9] The reaction with O_2 as oxidant is often time-consuming as it requires several hours for producing 70-80% of BINOL.[25,28] Therefore, the current interest in such process has been driven towards the synthesis of a new catalyst for obtaining BINOL using H_2O_2 as a suitable oxidant.[9] But the challenges remain in getting BINOL without any other hydroxyl or quinone derivatives of 2-naphthol.

Another academically and industrially important reaction is the benzylic C-H bond activation for the oxidation of benzylic alcohols to benzaldehydes eliminating the free radical mechanism.[1-4,29-32] The reaction is although quite common, but limiting the oxidation route strictly to benzaldehyde in the presence of oxidants like H_2O_2 or tetra-butyl hydrogen peroxide (TBHP) is still a difficult task.[29,33] Hence, in recent times, a large number of works has been devoted for such conversion accompanied by benzylic C-H bond activation.[1-4,29,33] One more challenging approach that has not been well recognized in the literature is the direct conversion of benzaldehyde to cinnamaldehyde by *in situ* generation of acetaldehyde (CH_3CHO) by ethanol (C_2H_5OH) oxidation. To the best of our knowledge, cinnamaldehyde is mostly produced by cross-aldol condensation of benzaldehyde with CH_3CHO in presence of a base like sodium hydroxide (NaOH) or potassium hydroxide (KOH).[34] Several other processes include Horner-Wadsworth-Emmons reaction,[35,36] Peterson reaction[37] and Wittig reaction.[38] Nordqvist *et al*. synthesized several derivatives of cinnamaldehyde by an oxidative Heck reaction between acrolein and phenylboronic acids.[39] However, the synthesis of cinnamaldehyde by *in situ* formation of CH_3CHO through partial oxidation of ethanol has not been reported so far in literature. As the cost of C_2H_5OH is lower than CH_3CHO, therefore the preparation of cinnamaldehyde through C_2H_5OH oxidation would be a highly economically viable process.

The above-stated reactions are completely different from one another and till now different types of catalysts are employed for individual reactions.[1,5,7,11,14] However, it would have been more advantageous if all the four reactions mentioned herein could have been promoted in the presence of a single catalyst. This, in turn, will reduce the time, cost and consumption of various transition metal-based catalysts during the synthesis of different catalysts for separate reactions. Apart from the synthesis of the catalyst with high activity, it is also an important aspect to look into the regeneration of the catalyst. In this regard, inorganic materials like zeolite-Y appeared as a suitable host-matrix for supporting metal-based nanocatalyst, providing a high surface area, alternating the acidity/basicity of the catalyst and more importantly, preserves the true heterogeneity of the nanocatalyst.[7,29,40,41] It also provides a high surface area framework and possesses a confinement effect, which are key factors in heterogeneous catalysis.[42-44] Therefore, looking at the need of a common heterogeneous catalyst, herein we report for a single Pd-Au-Y catalyst that can activate multiple reactions under different reaction conditions.

2. EXPERIMENTAL SECTION

2.1. Materials. Palladium chloride ($PdCl_2$) and gold (III) chloride ($AuCl_3$) were purchased from Merck and Sigma Aldrich and used as sources of palladium and gold, respectively. All the starting materials for SMCC reaction, 2-naphthol oxidation, oxidation of benzylic alcohol (OBA) and cinnamaldehyde synthesis were obtained from Sigma Aldrich. Tetra-n-butyl ammonium bromide (TBAB) was procured from E-Merck. C_2H_5OH and CH_3CN which were employed throughout the one-pot OBA-SMCC were purified prior to their use and deionized water was used for synthesis. All other solvents used in different reactions were purchased from E-Merck. All the bases for cinnamaldehyde synthesis were also procured from Merck and Sigma Aldrich.

2.2. Physical Measurements. X-ray diffraction (XRD) of the sample was measured in a Philips PANalytical Empyrean instrument, enabling low angle measurement from 0-60° with a minimum step size (2θ) of 0.0001. A UV-visible diffuse reflectance spectrum (UV-DRS) was obtained in a DR apparatus equipped with an assimilating sphere having 60 mm inner diameter, (Hitachi U-3400 spectrophotometer). To minimize the effect caused by fluorescence, a monochromatic light was employed in the full spectral range. The finely ground sample was then placed in a 10 mm diameter and 3 mm deep sample holder. The obtained film was considered to be infinitely thick as required in the Kubelka-Munk (K-M) theory of reflectance. Reflectance mode was set up in order to record the optical spectra and the KM study was achieved on the reflectance data providing the necessary data to perform the K-M analysis. Scanning electron microscopy (SEM) and electron-dispersive X-ray spectroscopy (EDS or EDX) mapping were done in JEOL, JAPAN, Model: JSM 6390LV. The transmission electron microscopy (TEM) images and the TEM-EDS were recorded on a JEOL (JEM-2010) instrument equipped with a CCD camera (slow-scan) with a 200 kV accelerating voltage. The X-ray photoelectron spectroscopy (XPS) of the sample was measured using Mg Kα (1253.6 eV) radiation as a source on a KRATOS (ESCA AXIS 165) spectrometer. The oven-dried samples (finely ground) were dusted on a graphite sheet (double stick) and mounted over the regular sample holder, before being transferred to an analysis chamber. Before recording the XPS, the material was outgassed overnight in a vacuum oven. The Raman analysis of the material was obtained in an EZRaman-N (Enwave Optronics) Raman Spectrophotometer, having laser light of 150 mW, 785 nm incident wavelength through 100x (0.3 N.A) objective lens. The N_2 adsorption-desorption data was obtained at 77 K in a NOVA 1000e, (Quantachrome Instruments) and the surface area was calculated by using the Brunauer–Emmett–Teller (BET) equation. Barret, Joyner, and

Halenda (BJH) pore diameter method was achieved from the desorption branch of the isotherm of the material. Catalytic conversions of alcohols to aldehydes and the product for SMCC reaction were confirmed *via* nuclear magnetic resonance (NMR) analysis using a 400 MHz NMR from JEOL, ECS-400. Fourier-transform infrared spectra (FT-IR) of the organic compounds were recorded on a Perkin-Elmer Spectrum 2000 FT-IR spectrometer in the range of 500-4000 cm^{-1}. The percentage of conversion and selectivity of benzylic alcohol oxidation were obtained from gas chromatography (GC) analysis with a CiC gas chromatography, 2010. The cyclic voltammetry (CV) studies were executed in CH Instruments potentiostat (CHI-600E meter). The high-performance liquid chromatography (HPLC) was recorded in instrument having specifications; model no. a) UV/Visible detector-2489, b) refractive index detector-2414, c) HPLC pump-525, Software: Empower-2, column: Symmetry ® C18 5 µm, 4.6 x 250 mm, column. Inductively Coupled Plasma (ICP) analyses were performed in PERKIN ELMER, USA, OPTIMA 2100 DV.

2.3. Synthesis of gold and palladium exchanged Zeolite-Y, Au-Y and Pd-Y. For synthesis of gold-exchanged zeolite-Y (Au-Y), a colloidal solution of gold (Au) was prepared following the reported procedure using amino acids as capping agent.[45,46] To a 100 mL solution of 10^{-4} M $AuCl_3$ prepared in Millipore water, 10 mg of sodium borohydride ($NaBH_4$) was added as a reducing agent in order to obtain a ruby-red coloured colloidal mixture. As used by Selvakannan *et al*.,[45] 0.5 mmol of lysine was added as a capping agent for stabilizing the Au-colloidal particles. From this stock colloidal solution of Au, 50 mL was pipetted out and mixed with 1 g of zeolite-NaY in a round bottom (RB) flask and refluxed for 20 h at 90 ^{o}C. The obtained material appearing pale violet in colour was consequently washed several times with hot distilled water. The $AgNO_3$ test was also performed in order to check the existence of excess chloride and was subsequently continued until a negative test was

obtained. Soxhlet extraction followed by centrifugation was performed to remove the excess lysine. The resultant material was then dried under argon for 6 h at 300 °C to obtain the final Au-Y material. The Pd-exchanged zeolite-Y (Pd-Y) was prepared as reported in our previous work.[7,29]

2.4. Synthesis of Pd-Au-Y in Zeolite-Y as support. The bimetallic Pd-Au-Y catalyst was prepared by drop-wise addition of 20 mL lysine-capped Au NPs colloidal solution (as synthesized in Au-Y) to the Pd-Y (Scheme 1). The subsequent mixture was continuously refluxed under nitrogen atmosphere for 24 h at 100 °C. The excess uncoordinated lysine was separated by performing a number of centrifugation cycles. The resultant Pd-Au-Y material was then dried under an argon atmosphere at 300 °C for about 12 h prior to its application. From the ICP analysis, the weight percentage (wt %) of Pd and Au in Pd-Au-Y were found to be 13.5 and 3.3 (mg/100 mg) respectively. This indicated that the wt % ratio of Pd:Au in the synthesized Pd-Au-Y catalyst was ~4:1.

2.5. Procedure for Suzuki-Miyaura Cross-Coupling (SMCC) Reaction. In a 50 mL RB flask containing 10 mL of water/ethanol (1:3), 3.2 mmol of phenylboronic acid (Ar-$B(OH)_2$) and 3 mmol of aryl chloride was added initially. To this mixture, 30 mg of Pd-Au-Y catalyst was added followed by the addition of 3 equivalents (equiv.) of cesium carbonate (Cs_2CO_3) and was further stirred for 10 minutes to dissolve the substrates and the base. The whole reaction mixture was then stirred for another 75 min at 80 °C to see the formation of biaryl. Hot filtration test was performed at different time intervals to determine whether there was any Pd leaching. Finally, the product was confirmed with ^1H and ^{13}C NMR and FT-IR analysis.

2.6. Procedure for Oxidation of 2-Naphthol. Oxidation of 2-naphthol was carried out by dissolving 2 mmol of substrate (2-naphthol) in 10 mL of distilled toluene. The solution was

then transferred to a 50 mL two-necked RB flask equipped with a condenser. After few minutes, 25 mg of Pd-Au-Y catalyst was added followed by the drop-wise addition 0.5 mmol of 30% H_2O_2. After the set-up, the whole reaction mixture was refluxed at 60 ^oC for 4 h. The progress of the reaction was monitored after an interval of 30 min with the help of thin layer chromatography. After 4 h of continuous stirring, the reaction was quenched and the catalyst was recovered by simple filtration. The recovered catalyst was then washed several times with ethyl acetate/hexane mixture, and dried in an oven at 80 ^oC for 12 h for further use. The same reaction was also carried out in a 50 mL two-necked RB flask equipped with a condenser and an air pump. The reaction was performed at 60 ^oC, with toluene as solvent, 25 mg of the catalyst for 11 h in reactor by passing a continuous flow of dry air. The flow of oxygen was controlled at the rate of 80 mL/min through a flow meter.

2.7. General Procedure for Oxidation of Benzylic Alcohol (OBA). All the OBA reactions were performed in a 50 mL RB flask under refluxing condition. At first, the RB flask was loaded with 30 mg of Pd-Au-Y catalyst followed by the addition of 2 mmol of benzylic alcohol (BA), 6 mL of HPLC grade CH_3CN as solvent and 10 mmol of H_2O_2 as oxidant. The temperature of the reaction mixture was maintained at 80 ^oC for 75 min over a digitally controlled magnetic stirrer. The catalyst was recovered by filtration technique. The % selectivity and % conversion was calculated from GC analysis. The product formation was further confirmed *via* ^1H and ^{13}C NMR analysis.

2.8. Procedure for One-pot OBA-SMCC Reaction. In a typical reaction, 5 mmol of p-chlorobenzyl alcohol, 4 mmol of Ar-$B(OH)_2$ was added in 50 mL RB flask containing 10 mL C_2H_5OH/CH_3CN as solvent system followed by H_2O_2 (20 mmol). To this mixture, 30 mg of the prepared Pd-Au-Y catalyst was added followed by the addition of 4 equiv. of a base

(Cs_2CO_3) and was further stirred for 75 minutes. The product was further confirmed *via* NMR and FT-IR analysis.

2.9. Procedure for Cinnamaldehyde Synthesis from Benzaldehyde. In a 50 mL RB flask, a mixture of 4 mmol of benzaldehyde and 5 mL of C_2H_5OH and 25 mg of Pd-Au-Y catalyst, 0.1 M NaOH solution was added slowly until the pH reached above 8. The whole reaction mixture was then refluxed at 120 ^oC for 4 h. After 4 h, the Pd-Au-Y was easily recycled by filtration. The catalyst was then washed many times with ethyl acetate/hexane mixture and dried overnight at 80 ^oC prior to its reuse.

2.10. Electrochemical Measurements. To understand the roles of Pd and Au in the multi-component reaction, a three-electrode system was employed using Ag/AgCl as a reference electrode, Pt wire as a counter electrode and glassy carbon as the working electrode, respectively. With the Pd-Au-Y catalyst drop cast over glassy carbon electrode, no electrochemical peaks were observed, so consequently, the CV studies were conducted in stirring conditions in C_2H_5OH/CH_3CN applying a scan rate of 100 mV/s.

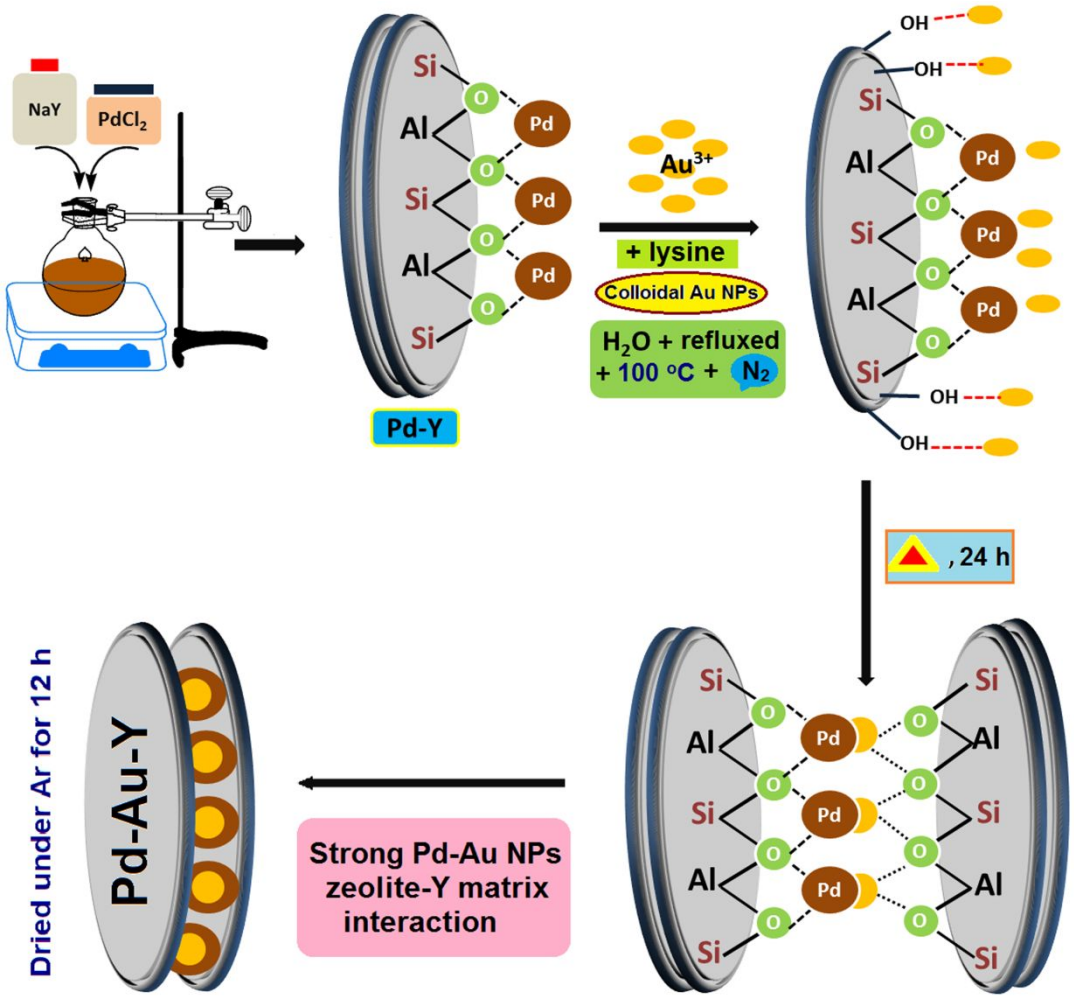

Scheme 1. Graphical representation of the synthesis method for the bimetallic Pd-Au-Y.

3. RESULTS AND DISCUSSION

After synthesizing the bimetallic catalyst, it was characterized by various analytical tools prior to its use in the catalytic application. Comparison of the XRD pattern of neat zeolite-Y and the Pd-Au loaded zeolite-Y suggested for the retention of the high crystallinity of zeolite-Y (Figure 1a). The appearance of the peaks at 2θ values of 38.2 and 44.3 in the XRD pattern (Figure 1a, red) corresponding to the (111) and (200) plane of bimetallic Pd-Au, clearly indicated the formation of a Pd-Au nanoalloy at the crystallite of zeolite-Y.[47,48] The peak intensities of the Pd-Au-Y were observed to be much higher than those of the pristine zeolite-Y. Such enhancement might result from surface modification caused by the

deposition of Pd and Au NPs.[29] The reversal of the peak intensities at 2θ values of 10 and 12 were ascribed to the diffusion of very low dimension Pd-Au NPs to the interior cavity of zeolite-Y during synthesis (Figure 1a, red).[7,29] The DRS of Pd-Au-Y was dominated by Pd NPs in the region of 300-400 nm (Figure 1b).[49,50] Usually, Au NPs show an LSPR band at ~520 nm, however, in the present case, this characteristic peak was found to be broad and weak.[49] This might result from the alloying of Au atom with Pd resulting in the transformation of the material from the original grey colour to light brown, (Figure 1b, inset).[49-51] A parallel observation was also found by Wang *et al*. with Pd-Au NPs supported on Mg-Al-layered double hydroxides (LDH).[52] Apart from these, two broad signals were observed above 600 nm. Pd NPs <10 nm are known to show their characteristic band below 400 nm (*i.e.* in the UV-region).[49,51] In this particular case, the shifting of the band to the visible range clearly indicated for NP-support interactions leading to the shifting of the band from the UV to the visible region. Hussain *et al*. also recently reported that Pd-particles below 10 nm supported over TiO_2 exhibited a band above 600 nm and showed activity as a water-splitting photo-catalyst.[53]

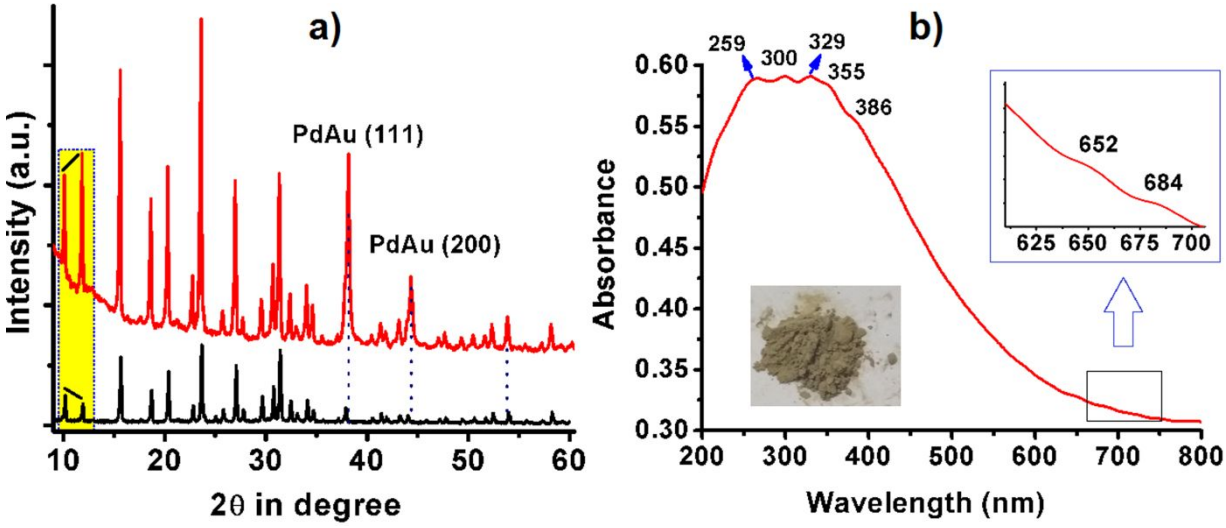

Figure 1. XRD pattern of a) Pd-Y (black) and Pd-Au-Y (red), b) DRS of Pd-Au-Y (inset shows the enlarged view from 625-700 nm).

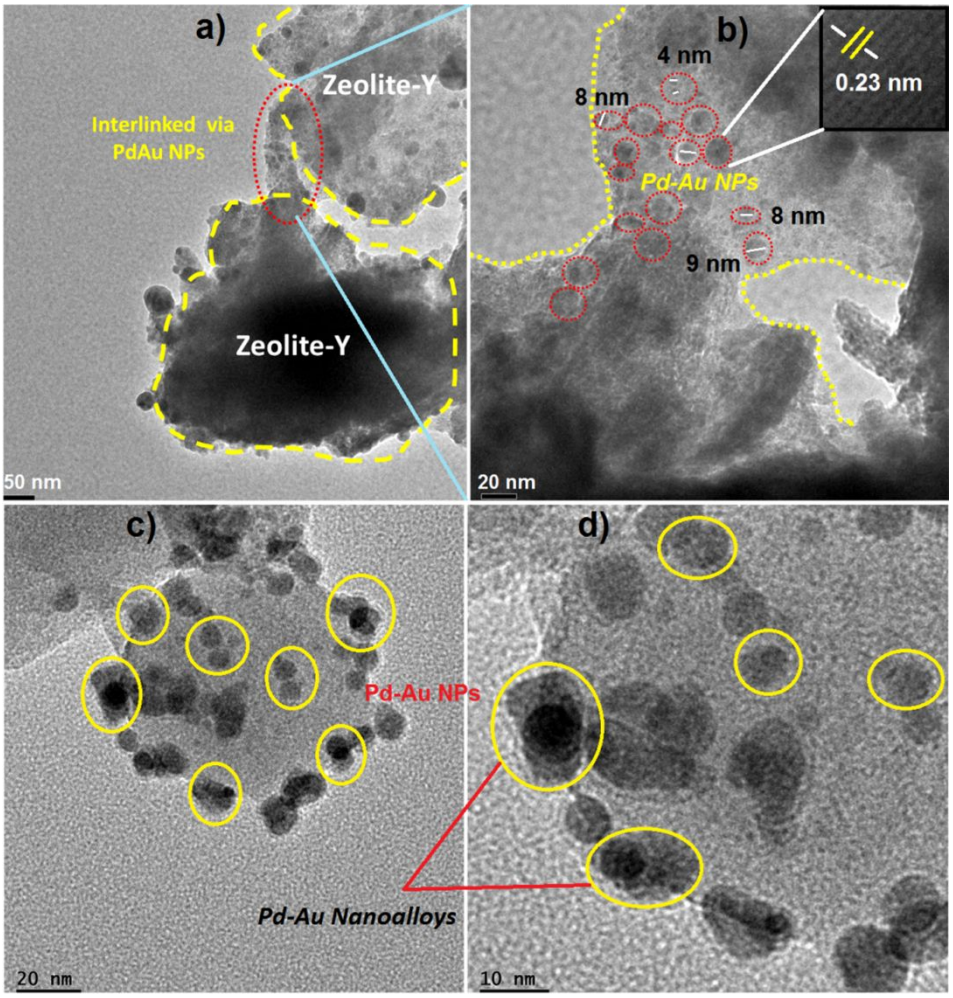

Figure 2. a-d) TEM images showing the interlinked zeolite-Y matrix of Pd-Au NPs (inset of Figure b shows the lattice fringe pattern of Pd-Au NPs).

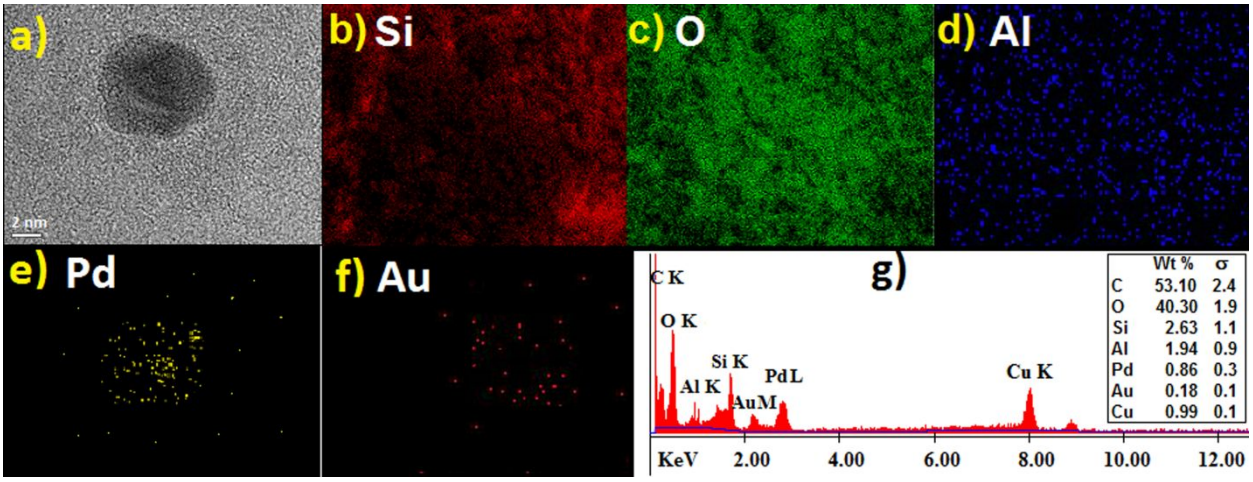

Figure 3. a) TEM image of Pd-Au nanoalloy considered for EDS elemental mapping of b) Si, c) O, d) Al, e) Pd, and f) Au. g) EDX spectra showing the presence of all the elements in Pd-Au-Y catalyst. The Cu and C contents were from the grid used for TEM analysis. The elemental amounts are given in wt %, sigma (σ) represents the error in elemental analysis.

The results obtained from DRS-spectral analysis were found to be in agreement with our TEM analysis showing the high dispersion of Pd-Au NPs <10 nm on the zeolite-Y crystallite (Figure 2 a-d). It was interesting to observe from the TEM analysis that the Pd-Au nanoalloys apart from forming at the zeolite-Y crystallite, the two zeolite crystallites were also found to be interlinked by these NPs (Figure 2a and 2b). Furthermore, the appearance of well-resolved lattice fringe having an inter-planar d-spacing value of ~0.23 nm also further ascertained the formation of Pd-Au nanoalloys (inset of Figure 2b). Similar lattice patterns were also observed by Hong *et al*. during the synthesis of Pd-Au nanowire.[54] The Pd-Au nanoalloys were mostly isolated without being agglomerated and the separation between them was within the range of 5-7 nm. The presence of such a small separation between the nanoalloys might result in a strong NP-NP interaction. This was also supported by a high red shift of Pd NPs absorption band and weakening of the characteristic LSPR band of Au NPs (Figure 1b). The presence of isolated nanoalloys of smaller dimension <10 nm further emphasize that the zeolite-Y acted as a good template for the decoration of small size Pd-Au nanoalloys. Previously also, other researchers including our group found that silicon-based matrices like MCM-41, zeolites and SBA-15 as suitable hard templating agent for preventing the agglomeration of small-sized NPs.[29,55,56] But to the best of our knowledge, Pd-Au nanoalloys are so far not synthesized in the zeolite-Y crystallite using the solid state dispersion (SSD) approach leading to highly ordered nanostructures. Therefore, SSD can be considered as a new greener approach for the synthesis of such nanoalloys.

Pd-Au nanoalloy formation on zeolite-Y was also ascertained from both TEM and SEM EDS/EDX analysis. The TEM-EDS mapping was performed selecting a single Pd-Au nanoalloy bound to the zeolite-Y support (Figure 3a). From this mapping analysis as shown in Figure 3 (b-f) and also from the EDX spectra (Figure 3g), it was confirmed that the Pd and

Au were present within the nanoalloys with a higher amount of Pd content. The presence of surface bound Pd-Au nanoalloy was also confirmed from the SEM-EDS analysis and are provided in supporting information, SI (Figure S1). In addition to this elemental analysis, XPS analysis on the sample was also performed to understand the nature of Pd and Au species supported on zeolite-Y. The binding energy (BE) region of Pd (3d) core level of Pd-Au-Y is shown in Figure 4a while that of Pd-Y is provided in SI (Figure S2a). The BE values for Pd in Pd-Au-Y were found to be ~335.0 eV and ~340.2 eV (spin orbit separation, Δ=5.2 eV) for Pd $3d_{5/2}$ and Pd $3d_{3/2}$, respectively while the same in case of Pd-Y was at 336.0 eV and 341.3 eV with Δ=5.3eV (Figure S2a).[5,47,57] The decrease in Pd (3d) BE in the Pd-Au-Y catalyst was attributed to the influence of Au on the electronic structure of Pd during the alloying process.[47,57] Similar BE values were also reported by various other researchers and was attributed to the formation of Pd (0) NPs.[5,47,57] In addition to these peaks, a very weak plasmon or satellite peak for PdO was observed at 337.8 eV.[58] The appearance of the satellite peak might result from the oxidation of Pd during X-ray irradiation. A similar plasmon band for PdO species was also observed by Holade *et al*.[58] with Pd nanomaterial's. The Au (4f) BE region in Pd-Au-Y and in Au-Y are shown in Figure 4b and Figure S2b, respectively. It showed a pair of peaks at 83.8 and 87.5 eV for Au $4f_{7/2}$ and Au $4f_{5/2}$, respectively which were found to be less in comparison to the Au-Y. These values were comparable with those of the Au (0) species observed in different forms of Au NPs.[59-62] Moreover, the spin orbit separation (Δ=3.7 eV) for Au was exactly matching with the reported results.[59-61] The XPS analysis thus signified that the Pd and Au in Pd-Au-Y were mostly in zerovalent oxidation state. The BE for Si 2p and Al 2p were found to be at 102.1, 103.1 and 74.5 eV indicating that the formation of Pd-Au nanaoalloy on zeolite-Y did not hampered the electronic configuration of Si and Al (Figure 4c and Figure 4d). No any peak for C 1s and N 1s was

detected in the XPS analysis suggesting the complete removal of capping agent (lysine) during the synthesis of the Pd-Au-Y catalyst. The ratio of Pd to Au (Pd:Au) from XPS analysis was found to be 4:1. As this ratio was matching with that of the ICP analysis, so it was considered to be the correct ratio.

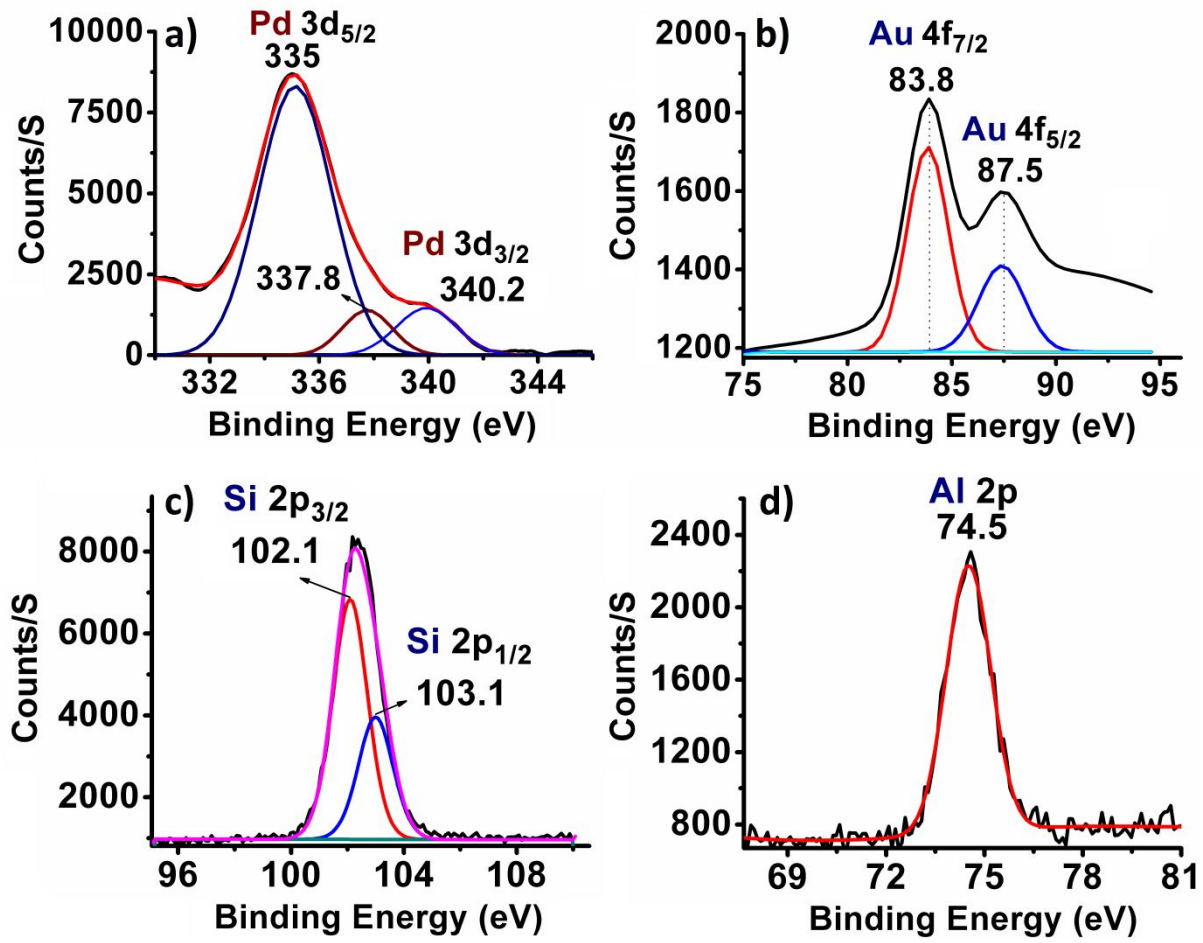

Figure 4. XPS spectra of a) Pd 3d, b) Au 4f, c) Si 2p and d) Al 2p in Pd-Au-Y catalyst.

Apart from the above analysis, the strong alloying of Au with Pd was also tested by treatment with acetic acid (CH_3COOH). The Pd-Y, Au-Y and Pd-Au-Y were treated individually with 0.1 M solution of CH_3COOH. The brown and yellow coloured solution of Pd and Au acetate respectively was observed on centrifuging the Pd-Y and Au-Y with CH_3COOH at 8000 rpm (Figure S3a and S3b, provided in SI). No any colour formation was resulted in similar treatment with Pd-Au-Y (Figure S3c). The results not only signified the

non-leaching property of Pd-Au nanoalloy in solution but also provided an experimental evidence for strong alloying of Au with Pd. Based on these experimental analyses, a plausible path for the formation of Pd-Au nanoalloy at the zeolite-Y surface is shown in Scheme 2.

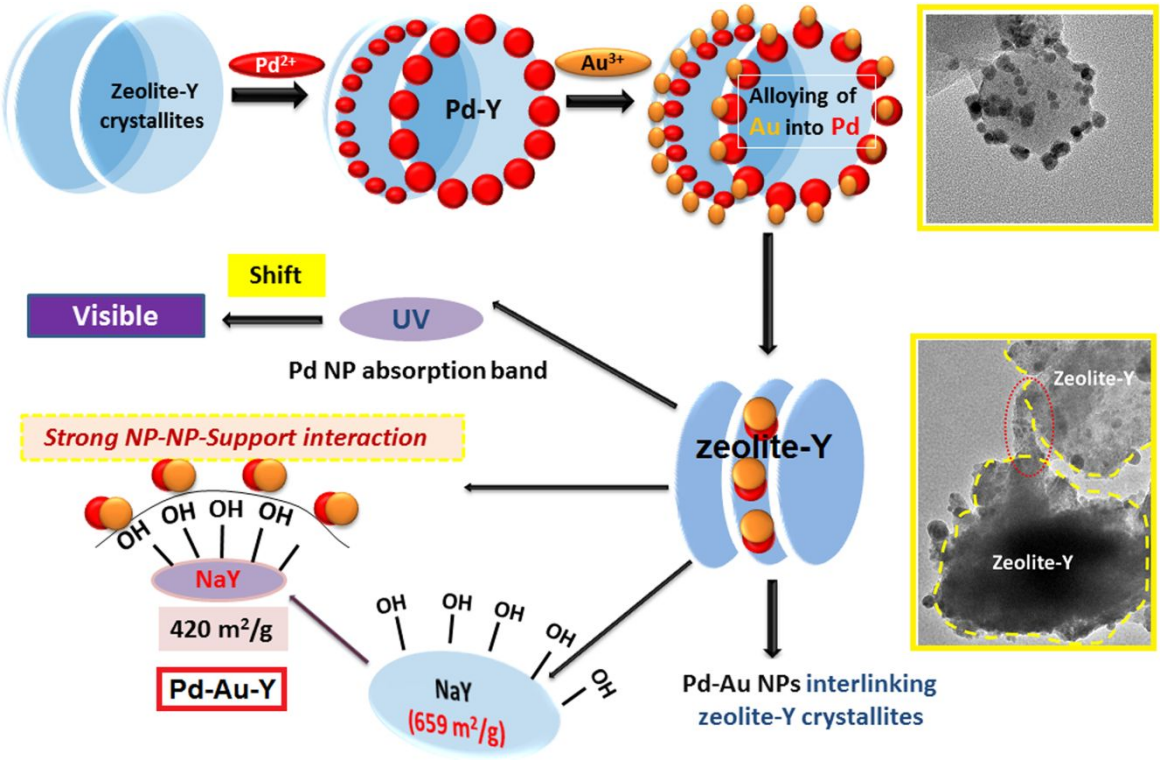

Scheme 2. Schematic representation demonstrating the probable interaction of Pd-Au NPs with the zeolite-Y (NaY) matrix.

Raman spectroscopy is one of the useful techniques for the investigation of metal oxide-based surfaces. Hence to further confirm the formation of Pd-Au nanoalloy at the zeolite-Y crystallite, Raman analysis was performed. In the Raman spectrum, a band at 228 cm^{-1} was ascribed to the lattice vibrations caused by the motion of the metal nanoclusters or metal cations.[63] The breathing mode vibration of four-membered rings of zeolite-Y was found to split into two bands at 484 and 531 cm^{-1} with substantial enhancement in intensity (Figure 5a).[7,63] In general, zeolite-Y exhibits a very weak breathing mode at 502 cm^{-1} in the Raman spectrum.[7,29,63] The splitting of bands was supposed to be caused by Fermi resonance. The result was found to resemble with those obtained with bimetallic Pd-NiO over zeolite-Y

matrix.[7] The band at 888 cm^{-1} could be attributed for the formation of Pd oxide surface due to some unalloyed Pd species.[64] Weak bands appearing at 1090 and 1354 cm^{-1} are ascribed to the Si-O stretching vibration associated with Al-O-Si bonds.[63]

The surface area of the synthesized material was determined from BET analysis and was found to be 420 m^2/g (Figure 5b). The drop in the surface area from 659 (neat zeolite-Y) to 420 (m^2/g) along with the pore size distribution (PSD) in the microporous and mesoporous region (1.8 to 2.6 nm) after modification with bimetallic Pd-Au NPs clearly provides supporting evidence of the presence of Pd-Au NPs at the zeolite-Y crystallite.[7,29,65]

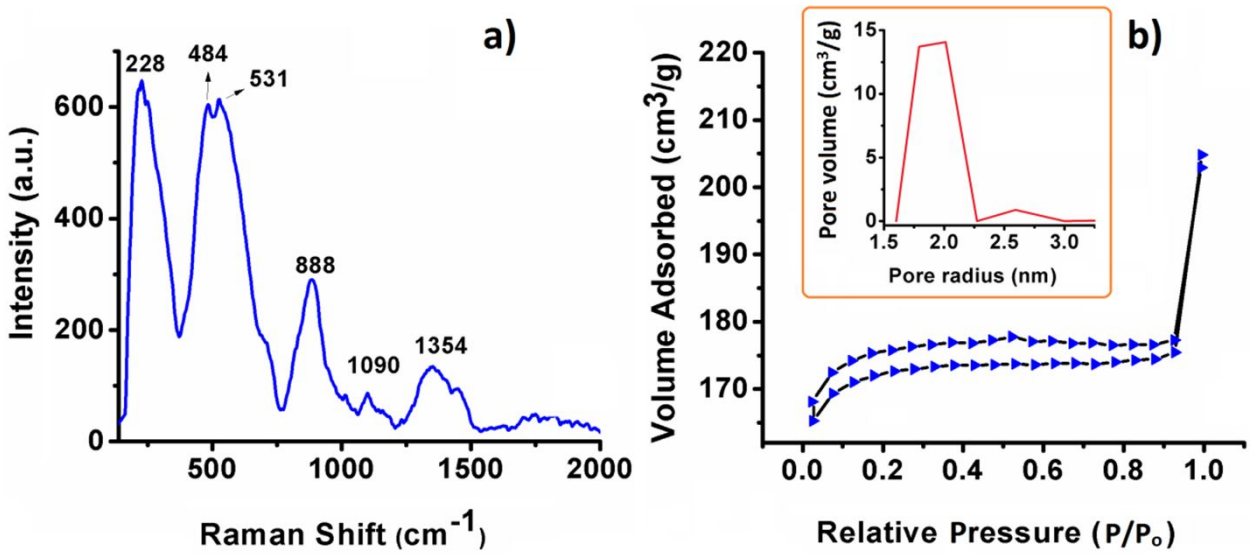

Figure 5. a) Raman spectra of Pd-Au-Y, (b) N_2 adsorption-desorption isotherm for Pd-Au-Y, with the inset showing the PSD curve.

3.1. Catalytic study: The main objective of this present work was to synthesize a suitable single catalyst that could manifest different types of catalytic reactions. In order to understand the ability of synthesized Pd-Au-Y catalyst, herein we have considered four important reactions namely, C-Cl bond activation, oxidation of 2-naphthol to BINOL with H_2O_2, benzylic C-H bond activation and direct conversion of aldehydes to cinnamaldehydes. The reason for choosing these four important reactions lies in the difficulties of C-Cl bond activation and selective synthesis of BINOL with H_2O_2.[7,9] Further, the development of new

and convenient synthetic approach for benzaldehydes and cinnamaldehydes preparation is highly demanding in fine chemical industries.[39] The reactions performed using the catalytic amount of Pd-Au-Y is discussed one by one in the following sections.

3.2. Suzuki-Miyaura Cross-Coupling (SMCC) Reaction. The SMCC reaction is considered as an important process for the construction of C-C bonds.[5,7,8,66,67] Nowadays, various metals like Au and Ni are amalgamated to Pd NPs to improve their catalytic activity owing to their synergistic effect.[5,7,8,67] Verma *et al*. demonstrated the efficiency of mesoporous silica supported Pd-Au NPs in carbon-halogen bond activation.[65] Therefore, Pd-Au-Y was used as a catalyst for SMCC reaction *via* activation of the C-Cl bond. The scope of the reaction was targeted only to chloro-substituted aryl halide as C-Br and C-I bonds are easy to activate even with Pd-salts.[20-22] From our previous studies,[7] it was found that C-Cl bond activation occurs effectively in water/ethanol (H_2O/C_2H_5OH) mixture (1:3). Therefore, without going for solvent optimization, SMCC reaction was performed using $ArB(OH)_2$ (3.2 mmol), *p*-chloro benzaldehyde (3 mmol) dissolved in a H_2O/C_2H_5OH solvent system (1:3), 30 mg of the Pd-Au-Y catalyst and 3 equiv. of Cs_2CO_3 as base at 80 ^oC. The results obtained under these conditions are depicted in Table 1. Thus, it was revealed that the Pd-Au-Y catalyst was able to activate the C-X (X=Cl) bond giving moderate to high percentage yield of biaryl products. The biaryl products were characterized by different spectroscopic analysis (NMR and FT-IR) and are provided in the SI. Under the present reaction condition, the C-Cl bond activation reaction was found to be sluggish with most of the substrates on performing the reactions with Pd-Y and Au-Y (Table 1). This implied that the alloying of Pd with Au was vital to improve its activity for effective C-Cl bond activation (Table 1). This was also in agreement with previous work where Pd-Y was found to be inactive for the activation of the C-Cl bond even in the presence of microwave radiation.[7] Sarina *et al.* also showed the

synergistic influence with respect to alloying of Pd-Au NPs for enhancing SMCC reaction.[67] Song *et al*. also showed the superior catalytic ability of Pd-Au core-shell NPs in Suzuki reaction.[68]

Table 1. SMCC reaction of phenylboronic acid with different aryl chloride using Pd-Au-Y catalyst conducted at 80 °C in H_2O/C_2H_5OH as the solvent.

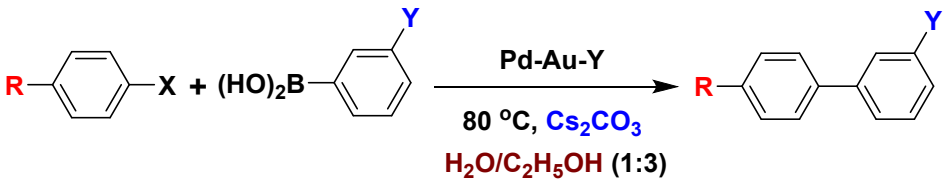

Entry	Substrate	Time (min)	Yield (%)		
			Pd-Y	Au-Y	Pd-Au-Y
1	**R**=H, **X**=Cl, **Y**=H	75	-	-	70
2	**R**=OCH_3, **X**=Cl, **Y**=NO_2	75	18	12	67
3	**R**=H, **X**=Cl, **Y**=NO_2	75	15	14	72
4	**R**=CHO, **X**=Cl, **Y**=H	75	-	-	73
5	**R**=CN, **X**=Cl, **Y**=H	75	-	-	71
6	**R**=CHO, **X**=Cl, **Y**=NO_2	75	16	16	76
7	**R**=OCH_3, **X**=Cl, **Y**=H	75	-	-	70
8	**R**=CH_3CO, **X**=Cl, **Y**=H	75	-	-	66

Reactions were run using derivatives of $ArB(OH)_2$ (3.2 mmol), 3 mmol of aryl chloride, 30 mg of Pd-Au-Y and 3 equiv. of Cs_2CO_3 in a mixture solvent of H_2O/C_2H_5OH (1:3).

3.3. Oxidation of 2-Naphthol to BINOL. As the Pd-Au-Y catalyst was found to be effective for C-C coupling reaction, the same catalyst was therefore employed for the C-C coupling of 2-naphthol to BINOL. Usually, iron or copper-based catalysts are used in presence of air or molecular oxygen (O_2).[10,11,25,26,28] There are several other catalysts that are also reported for synthesis of such chiral auxillaries.[10,11,25-28] The difficult part of this particular reaction is the controlled oxidation of 2-naphthol to BINOL, as the reaction is always hampered by the existence of other side products like 1,2-dihydroxynaphthalene and 1,2-naphthoquinone.[26,28]

Further, the reaction is very selective to solvent and oxidant.[11,26,28] The coupling reaction of 2-naphthol was found to be effective in presence of air or O_2 as an oxidant in chlorinated solvent or toluene.[11,26,28] Hence, challenges remains in the selective conversion of 2-naphthol to BINOL using H_2O_2 as an oxidant. Naya *et al*. reported for the selective oxidation of 2-naphthol to BINOL with $Au/SrTiO_3$-H_2O_2 based catalyst.[9] The catalyst was although selective towards BINOL formation but they studied the catalytic performance in micromolar (μmol) level. Narute *et al*. also performed asymmetric coupling of 2-naphthol using chiral Fe (III) catalyst with tertiary butyl peroxide (t-BuOOt-Bu).[10] Therefore, the search for a particular catalytic system that would allow a high yield of BINOL in presence H_2O_2 is still an ongoing process. Intrigued by the problem and challenges associated with this reaction in the presence of H_2O_2, the catalytic oxidation of 2-naphthol was performed with Pd-Au-Y catalyst.

From the literature, it was evident that the reaction preceded well in dichloromethane (CH_2Cl_2) or toluene.[11,26,28] Considering CH_2Cl_2 (10 ml) as the suitable solvent, the reaction was performed using 2 mmol of 2-naphthol, 10 mg of Pd-Au-Y and 0.5 mmol of H_2O_2 at room temperature. No conversion was observed up to 1 h, however, there was a slight decrease (3%) in 2-naphthol concentration due to surface adsorption.[11] The reaction was then run for another 3 h and fortunately, BINOL was obtained selectively without any other byproduct. The extracted yield of BINOL was 28% and increasing the reaction time did not improve the product yield and hence was not continued further. The C-C coupling of 2-naphthol is known to be influenced by catalyst amount, solvent system, temperature, and oxidant.[11,26,28] Therefore, keeping the reaction time to be fixed for 4 h and H_2O_2 amount as 0.5 mmol, the other reaction parameters were varied. On variation of the catalyst amount from 10 to 30 mg, the % yield of BINOL was found to be 46% on using 25 mg of Pd-Au-Y.

Under the same condition, BINOL was achieved up to 49% in toluene and 42% in CCl_4. Hence CH_2Cl_2, toluene and carbon tetrachloride (CCl_4) were found to be the suitable solvents for 2-naphthol oxidation with H_2O_2 as oxidant. The reaction was very non-selective in a polar solvent like C_2H_5OH, methanol (CH_3OH) and water leading to a mixture of products and was henceforth discarded. On varying the temperature from room temperature (20 ^oC) to 90 ^oC and keeping all other conditions same, the yield was improved to 58% in toluene, 56% in CH_2Cl_2 and 52% in CCl_4 at 60 °C (Figure S4a). Increasing the temperature above 60 ^oC dropped the selectivity of the reaction (Figure S4a) and at 90 ^oC mixtures of BINOL and 1,2-dihydroxynaphthalene and 1,2-naphthoquinone was obtained. The isolated % yield of BINOL, 1,2-dihydroxynaphthalene and 1,2-naphthoquinone found after performing the reaction in various solvents using these conditions are presented in Table 2. The reaction was also found to be highly dependent on H_2O_2 amount.[11,26] On increasing the H_2O_2 amount from 0.1 mmol to 0.5 mmol at 60 ^oC in toluene with 25 mg of Pd-Au-Y, % of BINOL formation also increases (Figure S4b). The reaction was well maintained up to 0.65 mmol, but overdosing of H_2O_2 up to 1 mmol reduced the % yield from 58% to 30% along with other side products (Figure S4b). Thus, from the above discussion, it was found that oxidation of 2-naphthol to BINOL was possible up to 58% yield using Pd-Au-Y catalyst in the presence of H_2O_2. However, there remained a large scope to improvise this particular reaction to achieve a better yield of BINOL.

Table 2. Catalytic oxidation of 2-naphthol using Pd-Au-Y with H_2O_2/O_2 at 60 °C.

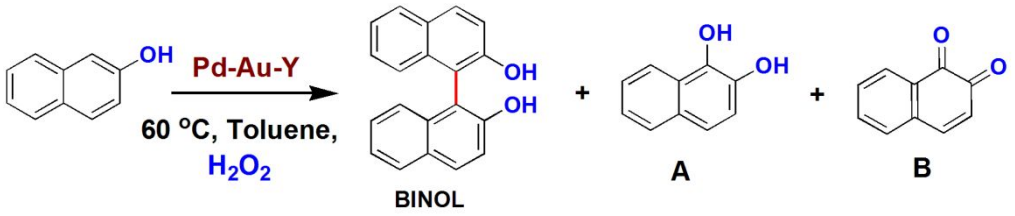

Solvent	Product yield (%) in H_2O_2			Product yield (%) in O_2		
	A	B	BINOL	A	B	BINOL
Ethanol	36	44	16	-	-	17
Methanol	35	48	10	-	-	12
Acetonitrile	42	37	14	-	-	21
CH_2Cl_2	-	-	56	-	-	65
Toluene	-	-	58	-	-	72
CCl_4	-	-	52	-	-	62

Reactions were carried out using 25 mg of Pd-Au-Y, 0.5 mmol H_2O_2 for 4 h at 60 °C, and with O_2 for 11 h with a flow rate of 80 mL/min. A=1,2-dihydroxynaphthalene; B=1,2-naphthoquinone

Although the oxidative coupling of 2-naphthol occurred in presence of Pd-Au-Y-H_2O_2 system, the reaction was very sensitive to solvent, temperature and peroxide amount and the yield was not so significant. The reaction was therefore again performed using O_2 as oxidant considering 25 mg of Pd-Au-Y and at 60 °C in toluene. The reaction was monitored as a function of the rate of O_2 flow. It was observed that the constant increase in O_2 flow from 10 mL/min up to 80 mL/min resulted in the successful formation of BINOL up to 72% without any byproduct (Figure S5). Previously, we also observed such dependency on the rate of oxygen flow or partial pressure of O_2 in the enantioselective oxidation of 2-naphthol using vanadium-Schiff base complex.[69] The reaction completion time with O_2 was more (11 h) in comparison to that in the presence of H_2O_2 (4 h). Considering this reaction time and the rate of oxygen flow as standard, the oxidation process was monitored in various solvents and the results are depicted in Table 2. It was observed that the reaction also proceeded without any byproduct in solvents like C_2H_5OH, CH_3OH and CH_3CN. The % yield of BINOL in the polar solvents was less in comparison to those in toluene and other chlorinated solvents

(Table 2). From the above analysis, it was thus ascertained that reaction with O_2 as oxidant was more advantageous in comparison to that with H_2O_2 *viz.* the product yield was high and the reaction was less sensitive to solvent. In the presence of H_2O_2, a small increment in H_2O_2 amount might change the whole story producing very less amount of BINOL. However, controlled oxidation of 2-naphthol to BINOL was achieved with moderate to good yield within a short period of time using 30% H_2O_2 as the green oxidant.[33] Since the reports on such oxidation process with H_2O_2 as oxidant is very sparse,[9,28] so we believe that Pd-Au-Y can be an effective catalyst for such non-preferential oxidation using H_2O_2. No BINOL formation was observed with Pd-Y and Au-Y either with H_2O_2 or O_2 as oxidant up to 72 h. The overall process of oxidation of 2-naphthol to BINOL can be represented as shown in Scheme 3.

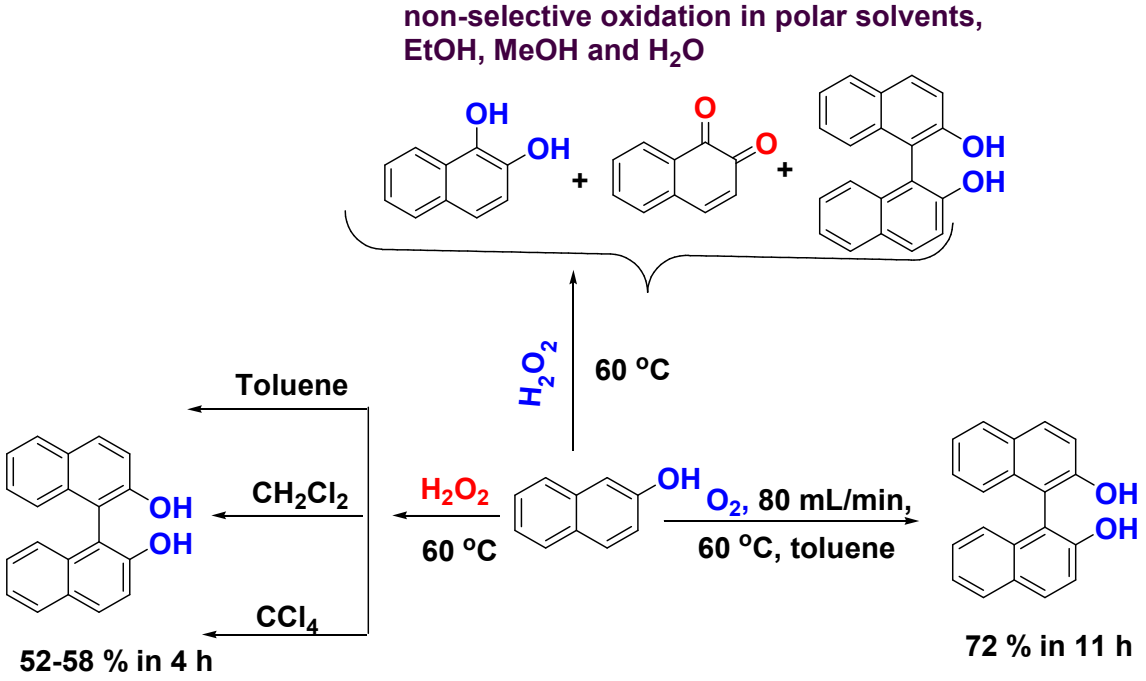

Scheme 3. Catalytic oxidation of 2-naphthol to BINOL in presence of H_2O_2 and O_2 with Pd-Au-Y catalyst.

3.4. Oxidation of Benzylic Alcohol (OBA). The OBA reaction was initially explored using 10 mg of the Pd-Au-Y catalyst, 2 mmol of the benzylic alcohol (as a test substrate), and 10

mmol of H_2O_2 at 40 ^oC in C_2H_5OH as the solvent for 1 h. Unfortunately, the obtained % conversions were very low and therefore the reaction was performed in different solvents keeping the other condition to be the same (Figure S6a). On the variation of the solvent, it was found that the reaction proceeded well in CH_3CN compared to many other solvents (Figure S6a). As the conversions and the selectivities were not satisfactory at 40 ^oC, therefore the reaction temperature was varied from 40 to 100 ^oC using CH_3CN as a solvent and all other conditions to be fixed (Figure S6b). On monitoring the temperature effect, the highest activity was found at 80 ^oC. As the catalyst amount also plays a dominant role in such reaction, consequently the catalyst amount was also varied from 10 to 50 mg and the results were found to be satisfactory with 30 mg of the catalyst (Figure S6c). Increase in the catalyst amount above 30 mg didn't alter the conversion and selectivity which might be due to the fact that 30 mg was the saturation level for the catalyst for this particular reaction. The effect of reaction time was also monitored at 80 ^oC using 30 mg of the catalyst in CH_3CN. The maximum conversion was observed on running the reaction for 75 min and no further increment was observed on increasing the reaction time (Figure S6d). Therefore, CH_3CN, 80 ^oC, 30 mg catalyst and 75 min was considered to be the standard conditions for the selective OBA to benzaldehyde. As different solvent responds differently to temperature and catalyst amount, so the OBA was again tested in various solvents, at 80 ^oC, and 30 mg of Pd-Au-Y (Table S1). The results were slightly different in comparison to that performed at 40 ^oC with 10 mg of the catalyst (Table S1). C_2H_5OH was found to be much comparable with CH_3CN, but the conversion and selectivity were slightly better in CH_3CN and hence was considered as the most suitable solvent system for OBA.

Table 3. Results for the OBA derivatives using CH_3CN as a solvent with Pd-Au-Y catalyst.

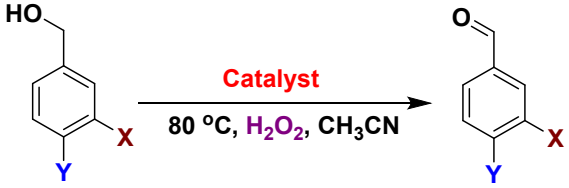

Entry	Substrate	Time (min)	(%) Conversion			(%) Selectivity		
			Pd-Y	Au-Y	Pd-Au-Y	Pd-Y	Au-Y	Pd-Au-Y
1	X, Y= H	75	21	24	73	>99	>99	>99
2	X=H, Y=Ar	75	25	28	75	>98	>98	>98
3	X=H, Y=NO_2	75	31	36	80	>98	>98	>98
4	X=H, Y=MeO	75	27	32	78	>98	>98	>98
5	X= NO_2, Y=H	75	26	34	76	>98	>98	>98
6	X=MeO, Y=H	75	20	39	71	>98	>98	>98
7	X=H, Y=Cl	75	21	28	74	>98	>98	>98
8	X=H, Y=F	75	17	19	68	>98	>98	>98

Reactions were implemented on a 2 mmol scale of benzylic alcohol derivative, 6 mL of CH_3CN, 10 mmol of H_2O_2 and 30 mg of Pd-Au-Y catalyst. GC-analysis was used to obtain the percentage conversion and selectivity.

After standardizing all the reaction parameter, the reaction was carried out with other alcohol substrates and the outcomes are presented in Table 3. For a better understanding of the reaction conditions, the bimetallic Pd-Au-Y catalyst was also compared with the monometallic zeolite-Y exchanged counterparts, Pd-Y and Au-Y. The catalytic conversions with all the substrates under identical conditions were found to be much improved with the Pd-Au-Y in comparison to the monometallic counterparts (Table 3). The obtained results clearly validated that the catalytic activity of the Pd towards selective OBA was influenced by Au and vice versa.[32] It is pertinent to mention herein that the percentage of conversion obtained herein with Pd-Y was less compared to the other reported results; however, the

results from the Au-Y were found to be in good agreement with other Au catalysts.[31,32] The difference in the catalytic performance of Pd-Y was attributed to the variation in reaction conditions and catalyst preparation technique.[32]

Table 4. Results for the one-pot OBA-SMCC reaction with Pd-Au-Y catalyst at 80 °C.

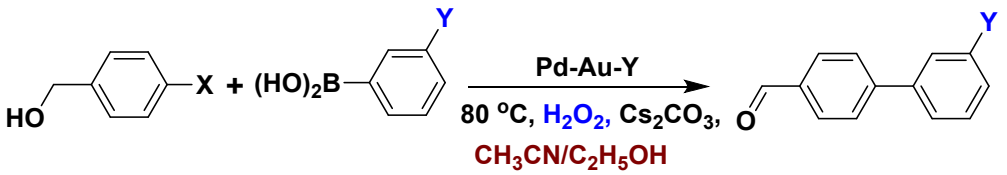

Entry	Substrate	Time (min)	Yield (%)		
			Pd-Y	Au-Y	Pd-Au-Y
1	**X**=Cl, **Y**= H	75	-	-	76
2	**X**=Cl, **Y**=NO_2	75	4	-	79
3	**X**=Br, **Y**=H	75	10	7	85
4	**X**=Br, **Y**=NO_2	75	22	16	87
5	**X**=I, **Y**=H	75	26	21	90
6	**X**=I, **Y**=NO_2	75	32	29	92

Reactions were run on a 5 mmol scale of X-benzylic alcohols and 4 mmol of phenylboronic acid, 10 mL of CH_3CN/ C_2H_5OH, 20 mmol of H_2O_2, Cs_2CO_3 (4 equiv.) and 30 mg of Pd-Au-Y catalyst.

3.5. One-pot OBA-SMCC Reaction. With the success in individual reaction and standard reaction parameters in hand, the Pd-Au-Y catalyst was employed for the synthesis of biaryl aldehyde derivative directly from X-benzylic alcohols (X=Cl, Br, I). The reactions were performed taking identical parameters i.e. 30 mg of catalyst, *p*-chloro benzylic alcohol (5 mmol), $ArB(OH)_2$ (4 mmol), H_2O_2 (20 mmol) as oxidant and Cs_2CO_3 (4 equiv.) in C_2H_5OH/CH_3CN solvent system at 80 °C. The results for the one-pot reaction are listed in Table 4. The mixture of C_2H_5OH /CH_3CN (3:1) solvent was employed in this reaction as this combination was found to be optimum and the results are shown in Table S2.

The percentage yield of biaryl derivative directly obtained from bromo/iodo substituted benzylic alcohols was almost comparable with those obtained with the chloro-substituted benzylic alcohol (Entries 4 and 6 in Table 4). Hence, it can be considered that biaryl aldehydes could be synthesized by activation of the benzylic C-H bond followed by successive C-X (X=Br, I, Cl) bond activation and C-C bond formation reactions, presenting an effective route for the synthesis of biaryl aldehydes starting from halo-substituted benzylic alcohols. In addition, it also provides a convenient approach to achieve multi-bond activation in a single-pot without the use of multistep work-up processes. The formation of biaryl aldehydes from benzylic alcohols was believed to occur through *in situ* oxidation of X-benzylic alcohols (X=Cl, Br, I) to corresponding aldehydes and its coupling with phenylboronic acid. To have better information on the assumption of *in situ* oxidation of X-benzylic alcohols, the samples were collected after an interval of 15 min to observe the presence of benzaldehyde, biaryl and also to see the change in the concentration of Cl-benzylic alcohol (Cl-BA). As the main objective of the present work was on C-Cl bond activation, so, this conversion was monitored taking Cl-BA as the test substrate. From the graph shown in Figure S7, it was observed that as the reaction progresses, there was a decrease in the concentration of Cl-BA. Up to 15-30 min, there was a certain concentration of Cl-benzaldehyde, but after 30 min, the concentration of biaryl aldehyde was sufficiently high indicating the coupling of the Cl-benzaldehyde resulted from the oxidation of Cl-BA with $ArB(OH)_2$.

This one-pot approach of synthesizing biaryl aldehydes from X-benzylic alcohols was expected to have certain advantages, i) aldehydes, especially the benzaldehydes are very sensitive to air producing the benzoic acids. So, this form of SMCC reaction that is selective for aldehyde formation would be beneficial in restricting the formation of over-oxidized

products, ii) usually the cost of benzylic alcohols is slightly higher in comparison to that of X-substituted benzaldehyde, therefore one might use directly the aldehydes for preparation of biaryl aldehydes. But in another way, starting with benzylic alcohol would be beneficial as it will reduce the cost and the time that will be spent for preparation of benzaldehyde from benzylic alcohols, one of the common techniques use for benzaldehyde preparation.[1-4] Recently, a sufficient number of studies has been made on the selective oxidation of benzylic alcohol to benzaldehyde using different transition metal-based catalyst.[1-4,29,33,40] As the Pd-Au-Y catalyst was highly selective for benzylic alcohol oxidation, therefore, from the industrial point of view it will be quite an effective process to look into such one-pot synthetic approach in SMCC type reaction.

3.6. Synthesis of Cinnamaldehyde from Benzaldehyde.

Cinnamaldehydes are considered to be one of the classical compounds that have high biological and pharmacological significance.[38,39] It has also found many applications as a flavoring agent, antimicrobial, antifungal compounds.[34,35,38] However, the synthesis of cinnamaldehydes is rather typical and its biosynthesis process involves a number of multiple steps using coenzymes.[70] Commonly known procedures for the synthesis of cinnamaldehydes are shown schematically in Scheme 4 along with the new and unknown approach adopted in this current study.

The % yield of cinnamaldehydes produced through condensation of CH_3CHO with benzaldehyde is comparatively not so prominent.[34] The process depends on how one adds the CH_3CHO to the benzaldehyde and also the pH of the media.[34,36] From the economic and industrial point of view, the synthesis of cinnamaldehyde by cross-aldol condensation is not a cost effective method as the price of CH_3CHO is reasonably high. Further, it is also difficult to have control over the oxidation of CH_3CHO to CH_3COOH. Looking at the price of the

CH_3CHO and its industrial importance, a large number of studies are now going on to obtain CH_3CHO from C_2H_5OH.[71] Various types of catalysts like Au-CuOx, Cu/ZrO_2 and $Au/MgCuCr_2O_4$ are reported to be active for complete or partial oxidation of C_2H_5OH.[71-73] Pd-Au catalysts are also known to be active for the oxidation of C_2H_5OH.[54,68] Thus, taking the advantage of Pd-Au-Y surface, herein we opted to synthesize various cinnamaldehydes by reaction of ortho and para substituted benzaldehyde with CH_3CHO formed by *in situ* partial oxidation of C_2H_5OH over Pd-Au-Y surface.

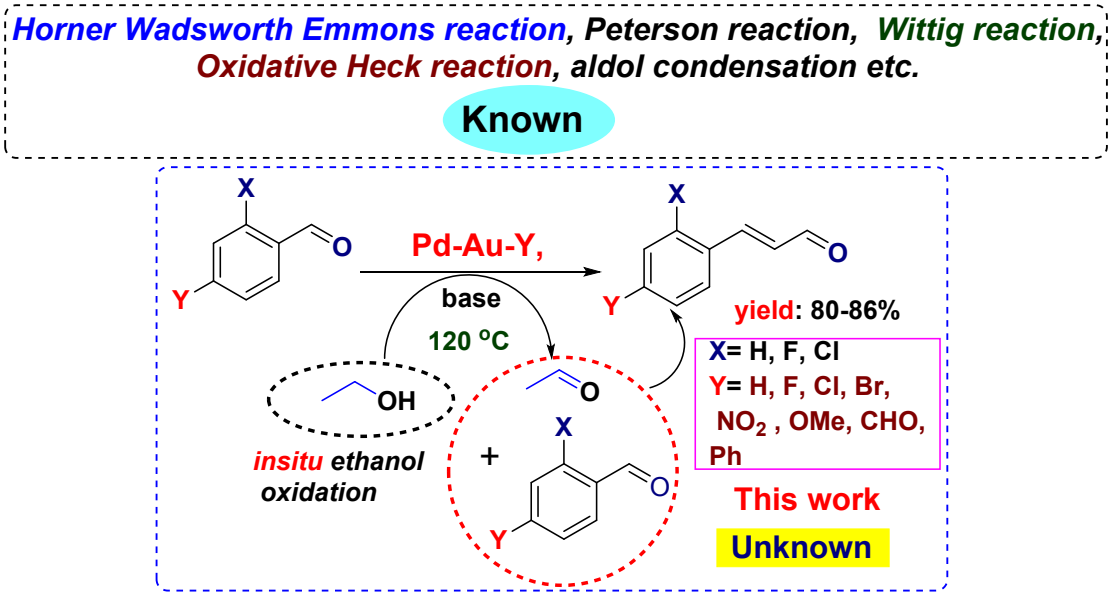

Scheme 4. Schematic representation showing known and unknown protocols for the synthesis of cinnamaldehydes.

The reaction was initially performed at 120 °C using 25 mg of Pd-Au-Y catalyst, 4 mmol of benzaldehyde and the cinnamaldehydes were obtained with very good yield (~80%) within 240 min (Entry 1, Table 5). The reaction was believed to be affected by temperature and catalyst amount, so the oxidation of C_2H_5OH and condensation with benzaldehyde was monitored at different temperatures and also by varying the catalyst amount. Taking 10 mg of Pd-Au-Y as constant catalyst amount, the reaction was performed at different temperatures and the results are plotted graphically (Figure S8a). The temperature was varied from 60 to

160 °C as most of the C_2H_5OH oxidation process occurs at high temperature i.e. above 200 to 250 °C.[71-73] No conversion was observed when the reaction was performed below 80 °C and the maximum yield was obtained at 120 °C (Figure S8a). Taking 120 °C as the standard temperature, we performed various other reactions by varying the catalyst amount from 10 to 30 mg (Figure S8b). The catalytic conversion was found to be the highest with 25 mg of the catalyst and there was no improvement in the reaction on increasing the catalyst amount to 30 mg (Figure S8b). The reaction was also monitored as a function of time (Figure S8c). The maximum yield of 80% was observed after running the reaction for 240 min and no further improvement was found on extending the reaction for another 40 min (Figure S8c). After standardizing the reaction condition, ten different cinnamaldehydes were produced by reacting the corresponding aldehydes with 25 mg of the catalyst, 5 mL of C_2H_5OH and at 120 °C for 240 min (Table 5).

The reaction was performed by adding a solution of (0.1 M) NaOH and maintaining the pH in between 8-11. The influences of different bases were also studied among which NaOH and KOH were found to be an excellent candidate for such aldol condensation reaction (Figure S8d). However, it should be mentioned herein that other bases like Cs_2CO_3 or K_2CO_3 also gave the same yield when the reaction was run for 24 h. As the reaction proceeded very fast in NaOH, so it was used for all the reactions. From the Table 5, it was observed that almost in all cases, more than 80% yield of the cinnamaldehydes were obtained with different substituted benzaldehyde. The formation of cinnamaldehyde was thus taken as a proof for the partial oxidation of C_2H_5OH to CH_3CHO in presence of Pd-Au-Y catalyst. As we have used 4 mmol of benzaldehyde (0.424 g) and 5 mL of C_2H_5OH (~4 g) and obtained 80% of cinnamaldehyde, so it was estimated that more than 0.32 g of CH_3CHO was generated from 4 g of C_2H_5OH during the aldol condensation process under the prevailing

condition. The formation of CH_3CHO was also tested by simply stirring C_2H_5OH with Pd-Au-Y using NaOH as base for 4 h. The presence of CH_3CHO in C_2H_5OH was confirmed from HPLC analysis recorded after 3 h (Figure S9).

Table 5. Results for cinnamaldehydes synthesis by cross-aldol condensation in C_2H_5OH at 120 °C.

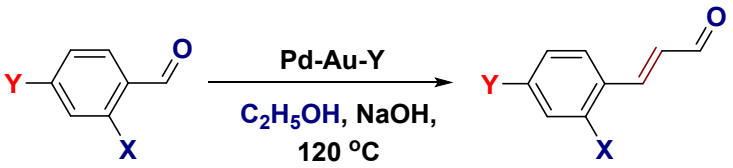

Entry	Substrate	% Yield[a]
1	X=H, Y=H	80
2	X=H, Y=F	77
3	X=H, Y=Br	83
4	X=H, Y=Cl	86
5	X=H, Y=NO_2	92
6	X=H, Y=OCH_3	87
7	X=F, Y=H	72
8	X=Cl, Y=H	78
9	X=H, Y=Ph	86
10	X=H, Y=CHO	82

Reactions were performed on a 4 mmol scale of benzaldehyde, 5 mL of C_2H_5OH, base and using 25 mg of Pd-Au-Y catalyst and all the reactions were stirred for 240 min. [a]Isolated yield

3.7. Comparison of Pd-Au-Y with the reported Pd-Au based catalysts in OBA and SMCC reactions. The reports on the selective oxidation of 2-naphthol to BINOL in H_2O_2 and also the preparation of cinnamaldehydes from benzaldehydes through *in situ* C_2H_5OH oxidation are very less known in literature.[9,10,34,35,39] Therefore, the comparative study of Pd-Au-Y was restricted only to OBA and SMCC reactions with various reported Pd-Au based catalysts.[74-87] The selective OBA with Pd-Au-Y catalyst was compared with some of the

reported results mentioned in Table 6. From the literature survey, it was found that most of the benzylic oxidation reactions using Pd-Au based catalysts were performed using O_2 as an oxidant to minimize the formation of the other side products like benzoic acid, benzylic ether, benzyl benzoate etc. (Table 6).[33] However, the O_2 as oxidant further requires a controlled experimental setup with sophisticated reactors controlling the partial pressure of oxygen. In this regard, 30% H_2O_2 appears to be a green oxidant that could be effectively used as a suitable oxidizing agent for OBA.[29,33] Recently, our group has found a Pd-CuO-Y based catalyst for the OBA using H_2O_2 as an oxidant.[29] As the reports on Pd-Au based catalyst on OBA using H_2O_2 are limited, so our approach of synthesizing the Pd-Au based nanocatalyst over NaY may be considered as an effective process for simple OBA giving the same conversion and selectivity. Similar to OBA, SMCC reaction (particularly C-Cl bond) with several Pd-Au based catalysts have also been compared with the synthesized Pd-Au-Y catalyst and are depicted in Table 6. On comparing, it was revealed that there are very few reports available for the activation of the C-Cl bond of the aryl halides in the SMCC reaction (Table 6). The SMCC processes were performed either *via* C-I or C-Br bond activation. Most of the reports also showed the use of different photo-catalytic reactors for such process. Liu *et al*.[88] showed the effect of Au doping over Pd for the successful cleavage of the C-Cl bond. To the best of our knowledge, though Pd-based catalyst has been extensively studied, the use of Pd-Au supported over zeolite-Y in the SMCC reaction has not been described in literature. So, designing a zeolitic based catalyst can be an effective method for the activation of the C-Cl bond in SMCC reaction by suppressing the side reactions and also enhancing the durability of the catalyst for restoring the active Pd-Au.

Table 6. Comparison of several reported Pd-Au based catalysts in the OBA and SMCC reactions.

OBA			SMCC			Ref
Catalyst	**Conditions**	**(%) Conv.**	**Catalyst**	**Conditions**	**(%) Yield**	
Pd_nAu/MSN	180 °C, pO_2, autoclave	60-90	PdAu-SBA	K_3PO_4, 100 °C, 30 min.	40-55	74, 75
Au@Pd NP	100 °C, pO_2, 2.5 h	14-87	Pd/Au/PN-CeO_2	K_2CO_3, 100 °C/h*v,* 6 h	15-88	76, 5
$(Au_x$-$Pd_y)$/C	120 °C, pO_2, 6 h	11-90	Au–Pd/TiO_2	K_2CO_3, RT, 5 h	14	77, 78
AuPdSBA-15	80 °C, pO_2, 2-8 h	10-39	Pd-Au-SBA-15	K_2CO_3, reactor, 4-8 h.	1-23	79, 65
AuPd-PANI	100 °C, pO_2, 3 h	99	Au-Pd/SiO_2	KOH, 80 °C, 2-4 h	39-59	32, 80
AuPd-TiO_2	100 °C, pO_2, 3-24 h	0.5	AuPd/MCM-41	KOH, 80 °C, 2-4 h	62-88	81, 80
Au/Pd	60 °C, pO_2, 3 h	32-96	AuPd-PVP	K_2CO_3, 27 °C, 24 h	50	82, 83
AuPd/TiO_2	100-160 °C, pO_2, 0.5 h	0.19-33.2	Au-Ag-Pd NP	CH_3COONa, 120 °C, 12 h	64-78	84, 85
AuPd/C/TiO_2	120 °C, pO_2, 0.5 h	61-81	Au-Pd NPs/GO	NaOH, 80 °C, 5 h	32-98	86, 87
Pd-Au-Y	80 °C, H_2O_2, 75 min	71-80	Pd-Au-Y	Cs_2CO_3, 80 °C, 75 min	67-76	This work

3.8. Understanding the Role of Pd and Au through Cyclic Voltammetry (CV) Studies. To comprehend the role of Pd and Au in the C-C coupling and benzylic C-H bond activation reactions, out of the four reactions, the one-pot synthesis of biaryl starting from Cl-BA was considered as a model reaction for the electrochemical study. Both the Pd and Au are known to be effective catalysts for OBA and SMCC reaction (Table 6). However, the individual role of Pd and Au in such a one-pot process is not well understood in literature. In most of the bimetallic catalysts, it is often stated about the synergism between the two metals that led to the improved catalytic activity of the nanocatalyst.[89] But, it is not always mandatory for the

existence of cooperativity between the two metal particles. In such cases, the two metal centers may behave individually without hampering the activity of each other. As in the present case, the activity of Pd-Y is being altered by introducing a low amount of Au and the material was found to activate the benzylic C-H bond as well as the C-Cl bond. Therefore, it is important to understand whether the activation was manifested by the synergism between the two metals or the individual metal was acting predominantly over one another.

In order to reveal the role of different species, the cyclic voltammograms were recorded for Pd-Au-Y catalyst with subsequent addition of the substrate. At the initial stage, a single cathodic peak was obtained at ~-1.02 V in the presence of Ar-$B(OH)_2$ and Cl-BA (Figure 6a). This was attributed to the reduction of the Pd (II) species of Pd-Au-Y to Pd (0).[7] The peak was found to retain when the CV was recorded in absence of Cl-BA (Figure 6b). This suggested that out of Pd and Au, Pd was more susceptible to interact with Ar-$B(OH)_2$ and has less affinity towards the Cl-BA. So, it was understood that although Pd and Au are known to activate benzylic C-H bond of aromatic alcohols, in a mixture of Ar-$B(OH)_2$ + Cl-BA, Pd will preferably interact with Ar-$B(OH)_2$. On increasing the amount of Cl-BA from 10 μL to 50 μL, the cathodic signal for Pd (II)/Pd (0) couple was found to get suppressed (Figure 6c).[7,90-94]As the amount of Cl-BA was increased to 50 μL, two anodic signals appeared at 0.55 V and 1.01 V corresponding to oxidation of Cl-BA and Au NPs, respectively (Figure 6d). The shift in the potential from 1.01 V towards more positive value on increasing the Cl-BA amount (60 μL to 100 μL) was attributed to the generation of more stable Au-oxide species (Figure 6d).

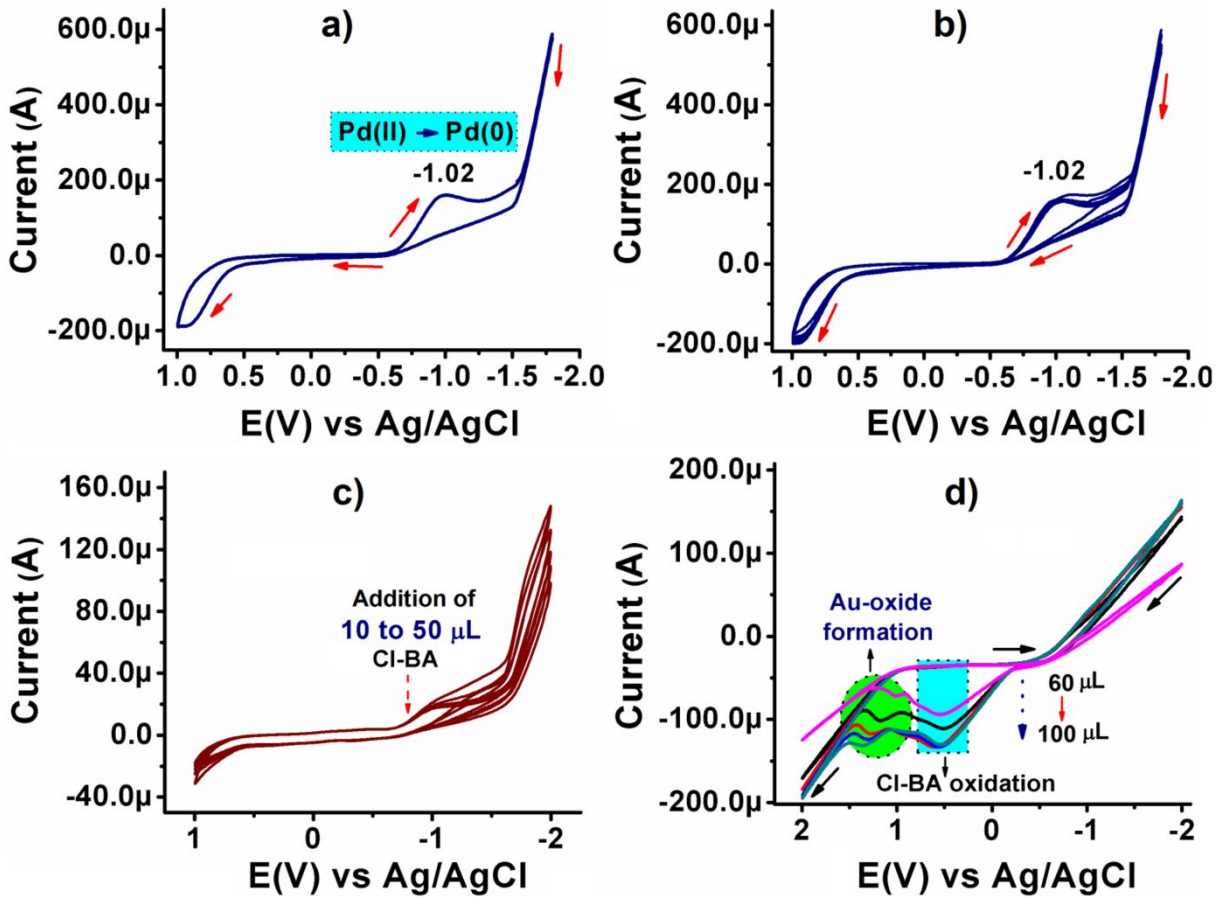

Figure 6. Cyclic voltammetry (CV) study of a) Pd-Au-Y + Ar-B(OH)$_2$ + Cl-BA, b) Pd-Au-Y + Ar-B(OH)$_2$ run for 10 consecutive cycles, c) Pd-Au-Y + Ar-B(OH)$_2$ + 4-Cl-BA (10 to 50 µL) and d) Pd-Au-Y + Ar-B(OH)$_2$ + 4-Cl-B.A (60 to 100 µL).

Cherevko *et al*. and Durovik *et al.* reported for the presence of peaks in the positive range (> 1 V) for the presence of various Au-oxides.[93,94] Zeis *et al.* also electrochemically showed the presence of Au-oxide at such positive potential range.[91] Furthermore, the disappearance of the reduction peak for Pd and the formation of additional oxidative signals clearly imply that the Au species interacts predominantly with the Cl-BA and thereby promotes its oxidation to the corresponding aldehyde. It might also happen that during the electrochemical generation of Cl-benzaldehyde, the Pd (0) species binds to the *in situ* generated aldehyde and therefore the oxidation peaks for Pd (0) to Pd (II) may not be observed in the cyclic voltammogram. In other words, the Pd (II) undergoes a reduction process to form Pd (0) active species and at the same time, Au NPs oxidizes the Cl-BA

thereby favouring the interaction of Cl-benzalaldehydes and Ar-$B(OH)_2$ with Pd (0) species to undergo an oxidative-reductive coupling to form biaryls. Thus, from the electrochemical studies, it was realized that the OBA will be mostly supported by Au species, while the Pd as usual actively participated in the coupling process.

3.9. Mechanism of one-pot OBA-SMCC Reaction. On the basis of CV analysis, a plausible mechanism is depicted in Scheme 5. At the first step, probably the oxidant, H_2O_2 interacts with the Au NPs forming a Au-peroxo like species (Scheme 5a).[92] The Cl-BA that gets adsorbed at the surface of zeolite-Y *via* weak H-bond then interacts immediately with the highly active and unstable Au-peroxo species (Scheme 5b). In this step, the hydroxyl proton of Cl-BA will eliminate as water and the resultant alkoxide intermediate will be bound to the AuO^+ species.[95,96] From the literature, it is well known that Pd species have the affinity for hydride transfer reaction and hence the Pd (0) species associated with the Au will promote the β-hydride transfer process forming the Cl-benzaldehyde (Scheme 5c).[95] In the CV analysis, it was also observed that there was no signal for oxidation of Pd (0) to Pd (II). This indirectly indicated for the high reluctant Pd (0) active species towards oxidation in presence of the substrates and probably this was favoured by the β-hydride transfer process. The hydride ion from the Pd-H was then supposed to be transferred to AuO^+ forming AuOH (Scheme 5d).[92] As the oxidation of AuO^+/AuOH species favours the generation of active Pd (0), the *in situ* generated species will also activate the C-Cl bond of Cl-benzaldehyde. In the CV, perhaps we observed the oxidation of AuO^+/AuOH to more stable oxides like Au_2O_3. After this, the other processes involved in the SMCC reaction will occur (Scheme 5e).[7] In the final reductive elimination step, the catalyst will be regenerated giving the biaryl aldehyde as the final product (Scheme 5f).

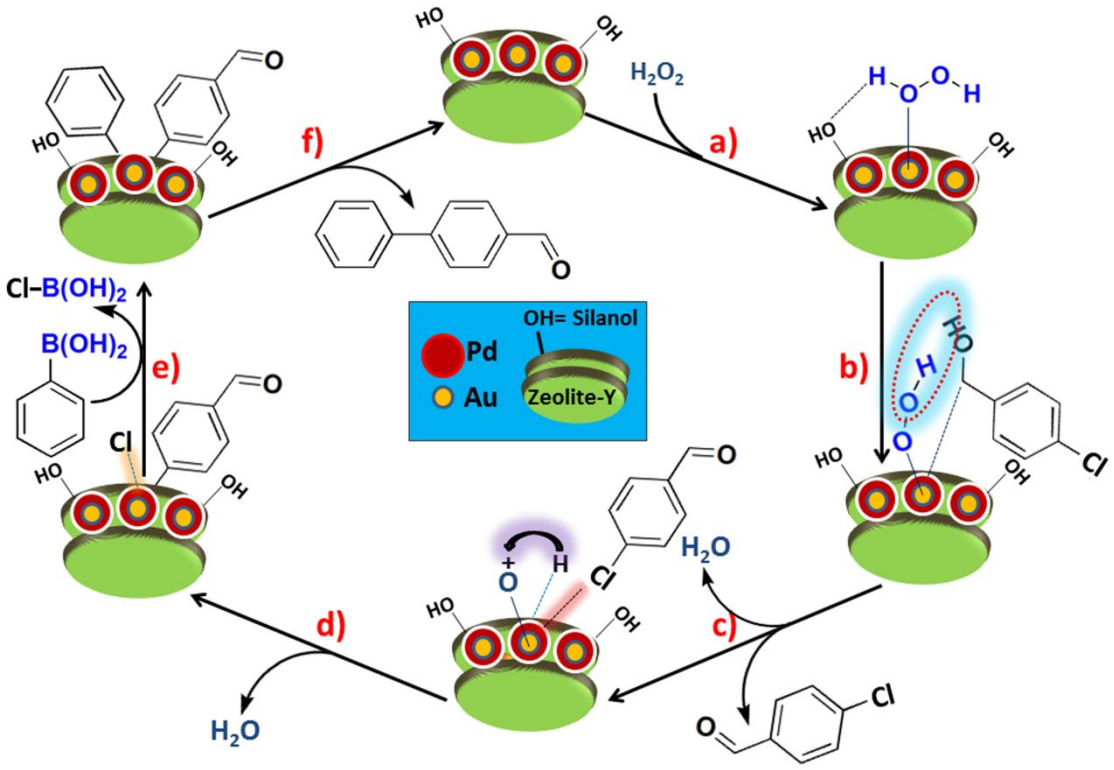

Scheme 5. A proposed mechanism of the one-pot reaction with Pd-Au-Y catalyst.

4. Recyclability of the Catalyst

Recyclability of catalysts without losing the active sites from the surface has been a never-ending task in the field of the heterogeneous catalyst. In this context, numerous attempts for designing various compact catalyst systems have been so far employed. In our case, Pd-Au-Y nanocatalyst was reused up to the 3rd cycle in OBA-SMCC reaction without having any effect on the % conversion. Up to the 3rd consecutive cycles, no leaching of metals was detected using the ICP analysis. The leaching of Pd was also tested by hot filtration test as reported by Jones group.[20-22] However, after the 3rd cycle, a significant decrease in the conversion rate occurred (Table S3). To diagnose the cut in the activity, TEM and XRD of the recovered catalysts were recorded in the 4th, 5th and 6th cycles. The XRD pattern of the Pd-Au-Y after the 3rd run was found to be slightly different from that of pristine Pd-Au-Y (Figure 7a) potentially resulting in the decreased catalytic activity. The TEM image (Figure 7b) and ICP analysis also revealed for the loss of Pd-Au NPs after the 5th cycle which

in turn resulted in the decrease in the catalytic performance. The recyclability test was also conducted in 2-naphthol oxidation as well in synthesis of cinnamaldehyde. In these two cases, the catalyst was also well recovered without any loss in activity up to six consecutive cycles. Thus Pd-Au-Y catalyst can be considered as an appropriate heterogeneous catalyst for performing different types of organic reactions with more or less similar activity.

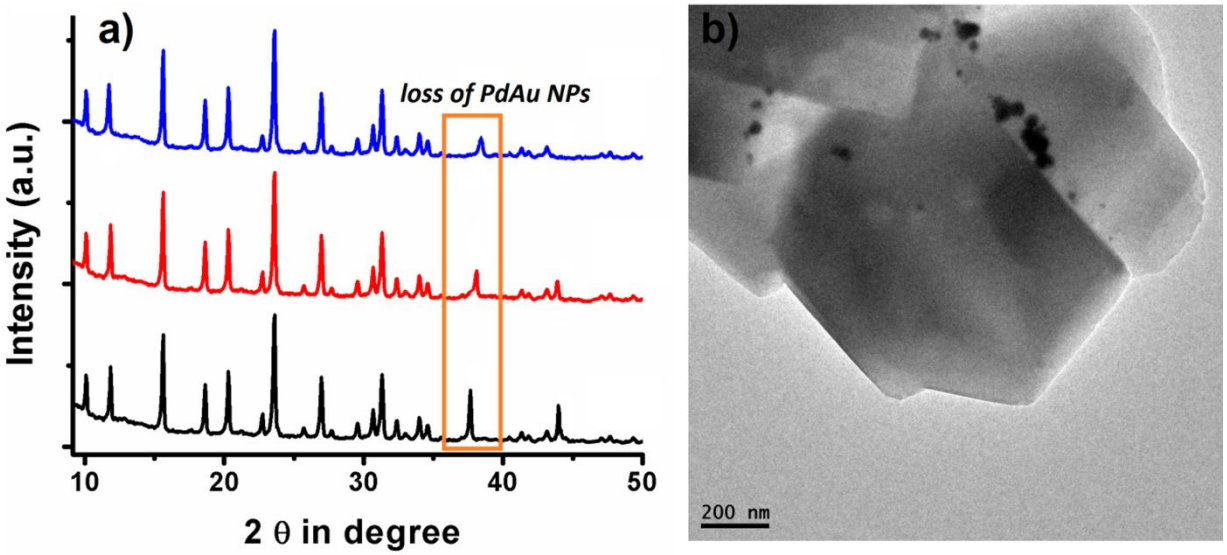

Figure 7. Recycled XRD pattern of the Pd-Au-Y taken for (a) 4th (black) 5th (red) and 6th (blue) runs after performing OBA-SMCC reaction and b) TEM image after 5th run.

5. Conclusion

In conclusion, it can be said that the Pd-Au nanoalloy supported over zeolite-Y matrix appeared as a useful catalyst for catalytic oxidation of 2-naphthols and benzylic alcohols. The high activity of the material and its ability to activate C-Cl bond in SMCC reaction can be considered as beneficial due to the low cost of the aryl chlorides. The most significant part of this catalyst was found in the oxidation of 2-naphthol to BINOL in presence of H_2O_2. More importantly, the production of cinnamaldehyde through C_2H_5OH oxidation might provide an economically viable method for the synthesis of cinnamaldehydes. To the best of our knowledge, there are very less amount of catalyst that could catalyze different type of reaction with similar activity. So, it is expected that such kind of catalytic approach in turn

will save the time and reduce the spent of other transition metals employed for individual catalytic reactions. In addition, the Pd-Au-Y catalyst was recyclable to number of cycles exhibiting itself as a true heterogeneous catalyst. This also implies the advantage of having zeolite-Y as a support for anchoring such nanoalloy.

ASSOCIATED CONTENT

Supporting Information

The supporting information includes XPS spectra of Pd-Y, Au-Y, optimization graphs and tables for the catalytic study in the oxidation of 2-Naphthol to BINOL reaction, OBA reaction, one pot OBA-SMCC reaction, synthesis of cinnamaldehyde from benzaldehyde, recyclability test of the one pot OBA-SMCC reactions. HPLC analysis of ethanol oxidation. ^{1}H, ^{13}C NMR of all the synthesized compounds and FT-IR spectra of the biaryls.

AUTHOR INFORMATION

Corresponding Author

*Email: kusum@tezu.ernet.in or bania.kusum8@gmail.com.

ORCID: 0000-0001-6535-3913

CONFLICTS OF INTEREST

There are no conflicts to declare.

ACKNOWLEDGEMENTS

MS and KKB acknowledge the Department of Science and Technology (DST), Science and Engineering Research Board, (SERB), India for the financial grant (NO SB/EMEQ-463/2014). MS also acknowledge CSIR-HRDG, New Delhi for the SRF fellowship (No 09/796(0094)/19-EMR-I). BD also thanks UGC-MHRD, Govt. of India for National Fellowship (RGNF-2017-18-SC-ASS-43132). The authors also thank Arup J. Das, Tezpur University for his support during analysis.

REFERENCES

(1) Fan, S.; Dong, W.; Huang, X.; Gao, H.; Wang, J.; Jin, Z.; Tang, J.; Wang, G. In Situ-Induced Synthesis of Magnetic Cu-$CuFe_2O_4$@HKUST-1 Heterostructures with Enhanced Catalytic Performance for Selective Aerobic Benzylic C–H Oxidation. *ACS Catal*. **2017**, *7*, 243−249.

(2) Zhao, G.; Yang, F.; Chen, Z.; Liu, Q.; Ji, Y.; Zhang, Y.; Niu, Z.; Mao, J.; Bao, X.; Hu, P.; Li, Y. Metal/Oxide Interfacial Effects on the Selective Oxidation of Primary Alcohols. *Nat. Commun*. **2017**, *8*, 14039.

(3) Chen, G. J.; Wang, J. S.; Jin, F. Z.; Liu, M. Y.; Zhao, C. W.; Li, Y. A.; Dong, Y. B. Pd@Cu(II)-MOF-Catalyzed Aerobic Oxidation of Benzylic Alcohols in Air with High Conversion and Selectivity. *Inorg. Chem*. **2016**, *55*, 3058−3064.

(4) Xie, Y.; Yang, Y.; Huang, L.; Zhang, X.; Zhang, Y. Pd-Catalyzed Arylation/Oxidation of Benzylic C-H Bond. *Org. Lett*. **2012**, *14*, 1238−1241.

(5) Zhang, S.; Chang, C.; Huang, Z.; Ma, Y.; Gao, W.; Li, J.; Qu, Y. Visible-Light-Activated Suzuki-Miyaura Coupling Reactions of Aryl Chlorides over the Multifunctional Pd/Au/Porous Nanorods of CeO_2 Catalysts. *ACS Catal*. **2015**, *5*, 6481−6488.

(6) O'Brien, H. M.; Manzotti, M.; Abrams, R. D.; Elorriaga, D.; Sparkes, H. A.; Davis, S. A.; Bedford, R. B. Iron-Catalysed Substrate-Directed Suzuki Biaryl Cross-Coupling. *Nat. Catal.* **2018**, *1*, 429–437.

(7) Sharma, M.; Sharma, M.; Hazarika, A.; Satyanarayana, L.; Karunakar, G. V.; Bania, K. K. C-Cl Bond Activation with Pd (II)-NiO Nanoparticles Supported on Zeolite-Y: The Role of Charge Transfer Transition. *Mol. Catal.* **2017**, *432*, 210–219.

(8) Biffis, A.; Centomo, P.; Zotto, A. D.; Zecca, M. Pd Metal Catalysts for Cross-Couplings and Related Reactions in the 21st Century: A Critical Review. *Chem. Rev*. **2018**, *118*, 2249−2295.

(9) Naya, S.; Hiramoto, Y.; Teranishi, M.; Tada, H. Room Temperature Selective Oxidation of 2-Naphthol to BINOL Using a $Au/SrTiO_3$-H_2O_2 Catalytic System. *Chem. Commun*. **2015**, *51*, 17669−17671.

(10) Narute, S.; Parnes, R.; Toste, F. D.; Pappo, D. Enantioselective Oxidative Homocoupling and Cross-Coupling of 2-Naphthols Catalyzed by Chiral Iron Phosphate Complexes. *J. Am. Chem. Soc*. **2016**, *138*, 16553−16560.

(11) Bania, K. K.; Bharali, D.; Viswanathan, B.; Deka, R. C. Enhanced Catalytic Activity of Zeolite Encapsulated Fe(III)-Schiff-Base Complexes for Oxidative Coupling of 2-Naphthol. *Inorg. Chem*. **2012**, *51*, 1657−1674.

(12) Ngo, D. T.; Tan, Q.; Wang, B.; Resasco, D. E. Aldol Condensation of Cyclopentanone on Hydrophobized MgO. Promotional Role of Water and Changes in the Rate-Limiting Step upon Organosilane Functionalization. *ACS Catal*. **2019**, *9*, 2831−2841.

(13) Young, Z. D.; Hanspal, S.; Davis, R. J. Aldol Condensation of Acetaldehyde over Titania, Hydroxyapatite, and Magnesia. *ACS Catal*. **2016**, *6*, 3193−3202.

(14) Zhang, J. F.; Wang, Z. M.; Lyu, Y. J.; Xie, H.; Qi, T.; Si, Z. B.; Liu, L. J.; Yang, H. Q.; Hu, C. W. Synergistic Catalytic Mechanism of Acidic-Silanol and Basic-Alkylamine Bifunctional Groups over SBA-15 Zeolite toward Aldol Condensation. *J. Phys. Chem. C* **2019**, *123*, 4903−4913.

(15) Kantam, M. L.; Srinivas, P.; Yadav, J.; Likhar, P. R.; Bhargava, S. Trifunctional N,N,O-Terdentate Amido/Pyridyl Carboxylate Ligated Pd(II) Complexes for Heck and Suzuki Reactions. *J. Org. Chem.* **2009**, *74*, 4882–4885.

(16) Dumbre, D. K.; Yadav, P. N.; Bhargava, S. K.; Choudhary, V. R. Suzuki–Miyaura Cross-Coupling Reaction Between Aryl Halides and Phenylboronic Acids over Gold Nano-Particles Supported on MgO (or CaO) and Other Metal Oxides. *J. Catal.* **2013**, *301*, 134–140.

(17) Zuo, Z.; Cong, H.; Li, W.; Choi, J.; Fu, G. C.; MacMillan, D. W. Enantioselective Decarboxylative Arylation of α-Amino Acids via the Merger of Photoredox and Nickel Catalysis. *J. Am. Chem. Soc*. **2016**, *138*, 1832−1835.

(18) Dander, J. E.; Garg, N. K. Breaking Amides using Nickel Catalysis. *ACS Catal*. **2017**, *7*, 1413−1423.

(19) Boit, T. B.; Weires, N. A.; Kim, J.; Garg, N. K. Nickel-Catalyzed Suzuki–Miyaura Coupling of Aliphatic Amides. *ACS Catal*. **2018**, *8*, 1003−1008.

(20) Richardson, J. M.; Jones, C. W. Strong Evidence of Solution-Phase Catalysis Associated with Palladium Leaching from Immobilized Thiols During Heck and Suzuki Coupling of Aryl Iodides, Bromides, and Chlorides. *J. Catal*. **2007**, *251*, 80−93.

(21) Phan, N. T.; Van Der Sluys, M.; Jones, C. W. On The Nature of the Active Species in Palladium Catalyzed Mizoroki–Heck and Suzuki–Miyaura Couplings Homogeneous or Heterogeneous Catalysis, A Critical Review. *Adv. Synth. Catal.* **2006**, *348*, 609−679.

(22) Richardson, J. M.; Jones, C. W. Poly (4-vinylpyridine) and Quadrapure TU as Selective Poisons for Soluble Catalytic Species in Palladium-Catalyzed Coupling Reactions–Application to Leaching from Polymer-Entrapped Palladium. *Adv. Synth. Catal*. **2006**, *348*, 1207−1216.

(23) Duan, L.; Fu, R.; Xiao, Z.; Zhao, Q.; Wang, J. Q.; Chen, S.; Wan, Y. Activation of Aryl Chlorides in Water under Phase-Transfer Agent-Free and Ligand-Free Suzuki Coupling by

Heterogeneous Palladium Supported on Hybrid Mesoporous Carbon. *ACS Catal.* **2014**, *5,* 575-586.

(24) Egami, H.; Matsumoto, K.; Oguma, T.; Kunisu, T.; Katsuki, T. Enantioenriched Synthesis of C 1-Symmetric BINOLs: Iron-Catalyzed Cross-Coupling of 2-Naphthols and Some Mechanistic Insight. *J. Am. Chem. Soc*. **2010**, *132*, 13633–13635.

(25) Meesala, Y.; Wu, H. L.; Koteswararao, B.; Kuo, T. S.; Lee, W. Z. Aerobic Oxidative Coupling of 2-Naphthol Derivatives Catalyzed by a Hexanuclear Bis(μ-hydroxo)copper(II) Catalyst. *Organometallics* **2014**, *33*, 4385−4393.

(26) Das, S. K.; Mahanta, S. P.; Bania, K. K. Oxidative Coupling of 2- Naphthol by Zeolite-Y Supported Homo and Heterometallic Trinuclear Acetate Clusters. *RSC Adv*. **2014**, *4*, 51496−51509.

(27) Kim, H. Y.; Takizawa, S.; Oh, K. Copper-catalyzed Divergent Oxidative Pathways of 2-Naphthol Derivatives: Ortho-Naphthoquinone *versus* 2-BINOLs. *Org. Biomol. Chem*. **2016**, *14*, 7191−7196.

(28) Wang, H. Recent Advances in Asymmetric Oxidative Coupling of 2-Naphthol and its Derivatives. *Chirality* **2010**, *22*, 827−837.

(29) Sharma, M.; Das, B.; Sharma, M.; Deka, B. K.; Park, Y. B.; Bhargava, S. K.; Bania, K. K. Pd/Cu-Oxide Nanoconjugate at Zeolite-Y Crystallite Crafting the Mesoporous Channels for Selective Oxidation of Benzyl-Alcohols. *ACS Appl. Mater. Interfaces* **2017**, *9*, 35453–35462.

(30) Layek, K.; Maheswaran, H.; Arundhathi, R.; Kantam, M. L.; Bhargava, S. K. Nanocrystalline Magnesium Oxide Stabilized Palladium (0): An Efficient Reusable Catalyst for Room Temperature Selective Aerobic Oxidation of Alcohols. *Adv. Synth. Catal*. **2011**, *353*, 606–616.

(31) Enache, D. I.; Edwards, J. K.; Landon, P.; Solsona-Espriu, B.; Carley, A. F.; Herzing, A. A.; Watanabe, M.; Kiely, C. J.; Knight, D. W.; Hutchings, G. J. Solvent-Free Oxidation of Primary Alcohols to Aldehydes using Au-Pd/TiO_2 Catalysts. *Science* **2006**, *311*, 362.

(32) Marx, S.; Baiker, A. Beneficial Interaction of Gold and Palladium in Bimetallic Catalysts for the Selective Oxidation of Benzyl Alcohol. *J. Phys. Chem. C* **2009**, *113*, 6191–6201.

(33) Das, B.; Sharma, M.; Kashyap, C.; Guha, A. K.; Hazarika, A.; Bania, K. K. Substrate Oxidation Prompted by Solvent Dissociation: The Role of Peroxo-Vanadate and Ag-π Interaction. *Appl. Catal., A* **2018**, *568,* 191–201.

(34) Richmond, H. H. Uniroyal Inc, Preparation of cinnamaldehyde. U.S. Patent 2, 529, 186, Nov 7, 1950.

(35) Blanchette, M. A.; Choy, Y.; Davis, J. T.; Essenfield, A. P.; Masamune, S.; Roush, W. R.; Sasaki, T. Horner-Wadsworth-Emmons Reaction: Use of Lithium Chloride and an Amine for Base-Sensitive Compounds. *Tetrahedron Lett*. **1984**, *25*, 2183-2186.

(36) Wadsworth, W. S. J.; Emmons, W. D. The Utility of Phosphonate Carbanions in Olefin Synthesis. *J. Am. Chem. Soc*. **1961**, *83*, 1733-1738.

(37) Ager, D. J. The Peterson Reaction. *Synthesis* **1984**, *5*, 384-398.

(38) Mackie, P. R.; Foster, C. E. Aldehydes: α, β-Unsaturated Aldehydes; Elsevier Pergamon: Amsterdam, London, 2005; Vol. 3.

(39) Nordqvist, A.; Björkelid, C.; Andaloussi, M.; Jansson, A. M.; Mowbray, S. L.; Karlen, A.; Larhed, M. Synthesis of Functionalized Cinnamaldehyde Derivatives by an Oxidative Heck Reaction and Their Use as Starting Materials for Preparation of *Mycobacterium tuberculosis* 1-Deoxy-d-xylulose-5-phosphate Reductoisomerase Inhibitors. *J. Org. Chem*. **2011**, *76*, 8986−8998.

(40) Lichen, L.; Corma, A. Metal Catalysts for Heterogeneous Catalysis: From Single Atoms to Nanoclusters and Nanoparticles. *Chem. Rev*. **2018**, *118*, 4981−5079.

(41) Sharma, M.; Das, B.; Hazarika, A.; Mangina, N. R.; Karunakar, G. V.; Bania, K. K. An Indirect Approach for Encapsulation of Chiral Cobalt Catalyst in Microporous Zeolite-Y. *Micropor. Mesopor. Mat*. **2018**, *272,* 31−39.

(42) Bania, K. K.; Karunakar, G. V.; Sarma, B.; Deka, R. C. Effect of Nanospace Confinement on the Catalytic Activity and Stability of a Chiral Schiff Base Complex (CuL; L= $C_{22}H_{24}N_2O_4$): A Combined Experimental and Theoretical Study. *ChemPlusChem* **2014**, *79*, 427−438.

(43) Cubillas, P.; Anderson, M. W. *In Zeolites and Catalysis: Synthesis, Reactions and Applications*, 1st ed.; Cejka, J., Corma, A., Zones, S., Eds.; Wiley-VCH: Weinheim, Germany, 2010; Vol. 1, pp 1-55.

(44) Sharma, M.; Das, B.; Karunakar, G. V.; Satyanarayana, L.; Bania, K. K. Chiral Ni-Schiff Base Complexes inside Zeolite-Y and their Application in Asymmetric Henry

Reaction: Effect of Initial Activation with Microwave Irradiation. *J. Phys. Chem. C* **2016**, *120*, 13563–13573.

(45) Selvakannan, P. R.; Mandal, S.; Phadtare, S.; Pasricha, R.; Sastry, M. Capping of Gold Nanoparticles by the Amino Acid Lysine Renders them Water-Dispersible. *Langmuir* **2003**, *19,* 3545−3549.

(46) Bhargava, S. K.; Booth, J. M.; Agrawal, S.; Coloe, P.; Kar, G. Gold Nanoparticle Formation during Bromoaurate Reduction by Amino Acids. *Langmuir* **2005**, *21*, 5949−5956.

(47) Tuo, Y.; Liu, G. F.; Dong, B.; Zhou, J. T.; Wang, A. J.; Wang, J.; Jin, R. F.; Lv, H.; Dou, Z.; Huang, W. Y. Microbial Synthesis of Pd/Fe_3O_4, Au/Fe_3O_4 and PdAu/Fe_3O_4 Nanocomposites for Catalytic Reduction of Nitroaromatic Compounds. *Sci. Rep*. **2015**, *5*, 13515.

(48) Sun, D. H.; Zhang, G. L.; Jiang, X. D.; Huang, J. L.; Jing, X. L.; Zheng, Y. M.; He, J.; Li, Q. B. Biogenic Flower-Shaped Au-Pd Nanoparticles: Synthesis, SERS Detection and Catalysis Towards Benzyl Alcohol Oxidation. *J. Mater. Chem. A* **2014**, *2,* 1767–1773.

(49) Sarina, S.; Bai, S.; Huang, Y.; Chen, C.; Jia, J.; Jaatinen, E.; Ayoko, G. A.; Bao, Z.; Zhu, H. Visible Light Enhanced Oxidant Free Dehydrogenation of Aromatic Alcohols Using Au–Pd Alloy Nanoparticle Catalysts. *Green Chem*. **2014**, *16*, 331−341.

(50) Zheng, Z.; Tachikawa, T.; Majima, T. Plasmon-Enhanced Formic Acid Dehydrogenation Using Anisotropic Pd−Au Nanorods Studied at the Single-Particle Level. *J. Am. Chem. Soc*. **2015**, *137*, 948−957.

(51) Mulvaney, P. Surface Plasmon Spectroscopy of Nanosized Metal Particles. *Langmuir* **1996**, *12*, 788−800.

(52) Wang, L.; Xu, N.; Pan, X.; He, Y.; Wang, X.; Su, W. Cobalt Lactate Complex as a Hole Cocatalyst for Significantly Enhanced Photocatalytic H_2 Production Activity over CdS Nanorods. *Catal. Sci. Technol.* **2018**, *8*, 1599−1605.

(53) Hussain, E.; Majeed, I.; Nadeem, M. A.; Badshah, A.; Chen, Y.; Nadeem, M. A.; Jin, R. Titania-Supported Palladium/Strontium Nanoparticles (Pd/Sr-NPs@P_{25}) for Photocatalytic H_2 Production from Water Splitting. *J. Phys. Chem*. *C* **2016**, *120*, 17205−17213.

(54) Hong, W.; Wang, J.; Wang, E. Facile Synthesis of Highly Active PdAu Nanowire Networks as Self-Supported Electrocatalyst for Ethanol Electrooxidation. *ACS Appl. Mater. Interfaces* **2014**, *6*, 9481–9487.

(55) Valkenberg, M. H.; Holderich, W. F. Preparation and use of Hybrid Organic–Inorganic Catalysts. *Catal. Rev*. **2002**, *44*, 321-374.

(56) Fajula, F.; Brunel, D.; Fajula, F.; Brunel, D. Unique Surface and Catalytic Properties of Mesoporous Aluminosilicates. *Micropor. Mesopor. Mater*. **2001**, *48*, 119-125.

(57) Carter, J. H.; Althahban, S.; Nowicka, E.; Freakley, S. J.; Morgan, D. J.; Shah, P. M.; Golunski, S.; Kiely, C. J.; Hutchings, G. J. Synergy and Anti-Synergy between Palladium and Gold in Nanoparticles Dispersed on a Reducible Support. *ACS Catal*. **2016**, *6*, 6623−6633.

(58) Holade, Y.; Canaff, C.; Poulin, S.; Napporn, T. W.; Servat, K.; Kokoh, K. B. High Impact of the Reducing Agent on Palladium Nanomaterials: New Insights from X-Ray Photoelectron Spectroscopy and Oxygen Reduction Reaction. *RSC Adv.* **2016**, *6*, 12627-12637.

(59) Lay, B.; Sabri, Y. M.; Ippolito, S. J.; Bhargava, S. K. Galvanically Replaced Au–Pd Nanostructures: Study of their Enhanced Elemental Mercury Sorption Capacity over Gold. *Phys. Chem. Chem. Phys.* **2014**, *16*, 19522−19529.

(60) Akolekar, D. B.; Bhargava, S. K. Investigations on Gold Nanoparticles in Mesoporous and Microporous Materials. *J. Mol. Catal. Chem*. **2005**, *236*, 77−86.

(61) Sudarsanam, P.; Selvakannan, P. R.; Soni, S. K.; Bhargava, S. K.; Reddy, B. M. Structural Evaluation and Catalytic Performance of Nano-Au Supported on Nanocrystalline $Ce_{0.9}Fe_{0.1}O_{2-\delta}$ Solid Solution for Oxidation of Carbon Monoxide and Benzylamine. *RSC Adv*. **2014**, *4*, 43460−43469.

(62) Li, R.; Kobayashi, H.; Tong, J.; Yan, X.; Tang, Y.; Zou, S.; Jin, J.; Yi, W.; Fan, J. Radical-Involved Photosynthesis of AuCN Oligomers from Au Nanoparticles and Acetonitrile. *J. Am. Chem. Soc.* **2012**, *134,* 18286-18294.

(63) Dutta, P. K.; Shieh, D. C.; Puri, M. Raman Spectroscopic Study of the Synthesis of Zeolite Y. *J. Phys. Chem*. **1987**, *91*, 2332−2336.

(64) Zhao, Z.; Elwood, J.; Carpenter, M. A. Phonon Anharmonicity of PdO Studied by Raman Spectrometry. *J. Phys. Chem. C* **2015**, *119*, 23094−23102.

(65) Verma, P.; Kuwahara, Y.; Mori, K.; Yamashita, H. Pd/Ag and Pd/Au Bimetallic Nanocatalysts on Mesoporous Silica for Plasmon-Mediated Enhanced Catalytic Activity under Visible Light Irradiation. *J. Mater. Chem. A* **2016**, *4*, 10142−10150.

(66) Sun, D.; Li, Z. Double-Solvent Method to Pd Nanoclusters Encapsulated inside the Cavity of NH_2−Uio-66(Zr) for Efficient Visible-Light-Promoted Suzuki Coupling Reaction. *J. Phys. Chem. C* **2016**, *120*, 19744−19750.

(67) Sarina, S.; Zhu, H.; Jaatinen, E.; Xiao, Q.; Liu, H.; Jia, J.; Chen, C.; Zhao, J. Enhancing Catalytic Performance of Palladium in Gold and Palladium Alloy Nanoparticles for Organic Synthesis Reactions through Visible Light Irradiation at Ambient Temperatures. *J. Am. Chem. Soc*. **2013**, *135*, 5793−5801.

(68) Song, H. M.; Moosa, B. A.; Khashab, N. M. Water-dispersable Hybrid Au–Pd Nanoparticles as Catalysts in Ethanol Oxidation, aqueous Phase Suzuki–Miyaura and Heck Reactions. *J. Mater. Chem.* **2012**, *22*, 15953–15959.

(69) Mandal, M.; Nagaraju, V.; Karunakar, G. V.; Sarma, B.; Borah, B. J.; Bania, K. K. Electronic, Conjugation and Confinement Effects on Structure, Redox and Catalytic Behavior of Oxido-Vanadium (IV) and (V) Chiral Schiff Base Complexes. *J. Phys. Chem. C* **2015**, *119*, 28854–28870.

(70) Koukol, J.; Conn, E. E. The Metabolism of Aromatic Compounds in Higher Plants IV. Purification and Properties of the Phenylalanine Deaminase of Hordeum Vulgare. *J. Biol Chem.* **1961**, *236,* 2692-2698.

(71) Hanukovich, S.; Dang, A.; Christopher, P. The Influence of Metal Oxide Support Acid Sites on Cu Catalyzed Non-Oxidative Dehydrogenation of Ethanol to Acetaldehyde. *ACS Catal.* **2019**, *9*, 3537–3550.

(72) Bauer, J. C.; Veith, G. M.; Allard, L. F.; Oyola, Y.; Overbury, S. H.; Dai, S. Silica Supported Au − CuO_x Hybrid Nanocrystals as Active and Selective Catalysts for the Formation of Acetaldehyde from the Oxidation of Ethanol. *ACS Catal*. **2012**, *2*, 2537-2546.

(73) Liu, P.; Hensen, E. J. M. Highly Efficient and Robust Au/ $MgCuCr_2O_4$ Catalyst for Gas-Phase Oxidation of Ethanol to Acetaldehyde. *J. Am. Chem. Soc.* **2013**, *135*, 14032−14035.

(74) Yang, X.; Huang, C.; Fu, Z. Y.; Song, H. Y.; Liao, S. J.; Su, Y. L.; Du, L.; Li, X. An Effective Pd-promoted Gold Catalyst Supported on Mesoporous Silica Particles for the Oxidation of Benzyl Alcohol. *J. Appl. Catal*., *B* **2013**, *140*, 419−425.

(75) Zheng, Z.; Li, H.; Liu, T.; Cao, R. Monodisperse Noble Metal Nanoparticles Stabilized in SBA-15: Synthesis, Characterization and Application in Microwaved-Assisted Suzuki−Miyaura Coupling Reaction. *J. Catal.* **2010**, *270*, 268−274.

(76) Silva, T. A.; Teixeira-Neto, E.; Lopez, N.; Rossi, L. M. Volcano-like behavior of Au-Pd Core-Shell Nanoparticles in the Selective Oxidation of Alcohols. *Sci. Rep*. **2015**, *4*, 5766.

(77) Pritchard, J.; Kesavan, L.; Piccinini, M.; He, Q.; Tiruvalam, R.; Dimitratos, N.; Lopez-Sanchez, J. A.; Carley, A. F.; Edwards, J. K.; Kiely, C. J.; Hutchings, G. J. Direct Synthesis of Hydrogen Peroxide and Benzyl Alcohol Oxidation Using Au-Pd Catalysts Prepared by Sol Immobilization. *Langmuir* **2010**, *26*, 16568−16577.

(78) Han, D. X.; Bao, Z. B.; Xing, H. B.; Yang, Y. W.; Ren, Q. L.; Zhang, Z. G. Fabrication of Plasmonic Au-Pd Alloy Nanoparticles for Photocatalytic Suzuki-Miyaura Reactions Under Ambient Conditions. *Nanoscale* **2017**, *9*, 6026−6032.

(79) Ma, C. Y.; Dou, B. J.; Li, J. J.; Cheng, J.; Hu, Q.; Hao, Z. P.; Qiao, S. Z. Catalytic Oxidation of Benzyl Alcohol on Au or Au−Pd Nanoparticles Confined in Mesoporous Silica. *Appl. Catal., B* **2009**, *92*, 202−208.

(80) Speziali, M. G.; Silva, A. G. M. Da.; Miranda, D. M. V. de; Monteiro, A. L.; Robles-Dutenhefner, P. A. Air Stable Ligandless Heterogeneous Catalyst Systems Based on Pd And Au Supported in SiO_2 and MCM-41 for Suzuki−Miyaura Cross-Coupling in Aqueous Medium. *Appl. Catal., A* **2013**, *462−463*, 39−45.

(81) Li, G.; Enache, D. I.; Edwards, J.; Carley, A. F.; Knight, D. W.; Hutchings, G. J. Solvent-Free Oxidation of Benzyl Alcohol with Oxygen using Zeolite-Supported Au and Au-Pd Catalysts. *Catal. Lett*. **2006**, *110*, 7−13.

(82) Dimitratos, N.; Villa, A.; Wang, D.; Porta, F.; Su, D.; Prati, L. Pd and Pt Catalysts Modified by Alloying with Au in the Selective Oxidation of Alcohols. *J. Catal.* **2006**, *244*, 113-121.

(83) Dhital, R. N.; Sakurai, H. Anomalous Efficacy of Bimetallic Au /Pd Nanoclusters in C-Cl Bond Activation and Formal Metathesis-type C-B Bond Activation at Room Temperature. *Chem. Lett*. **2012**, *41*, 630−632.

(84) Miedziak, P. J.; He, Q.; Edwards, J. K.; Taylor, S. H.; Knight, D. W.; Tarbit, B.; Kiely, C. J.; Hutchings, G. J. Oxidation of Benzyl Alcohol Using Supported Gold−Palladium Nanoparticles. *Catal. Today* **2011**, *163*, 47−54.

(85) Venkatesan, P.; Santhanalakshmi, J. Synthesis, Characterization and Catalytic Activity of Trimetallic Nanoparticles in the Suzuki C–C Coupling Reaction. *J. Mol. Catal. Chem.* **2010**, *326*, 99-106.

(86) Tiruvalam, R. C.; Pritchard, J. C.; Dimitratos, N.; Lopez-Sanchez, J. A.; Edwards, J. K.; Carley, A. F.; Hutchings, G. J.; Kiely, C. J. Aberration Corrected Analytical Electron Microscopy Studies of Sol-Immobilized Au Plus Pd, Au{Pd} and Pd{Au} Catalysts Used for Benzyl Alcohol Oxidation and Hydrogen Peroxide Production. *Faraday Discuss*. **2011**, *152*, 63–86.

(87) He, Y.; Zhang, N.; Zhang, L.; Gong, Q.; Yi, M.; Wang, W.; Qiu, H.; Gao, J. Fabrication of Au–Pd Nanoparticles/Graphene Oxide and their Excellent Catalytic Performance. *Mater. Res. Bull.* **2014**, *51*, 397-401.

(88) Liu, R.; Zhao, H.; Zhao, X.; He, Z.; Lai, Y.; Shan, W.; Bekana, D.; Li, G.; Liu, J. Au@Pd Bimetallic Nanocatalyst for Carbon–Halogen Bond Cleavage: An Old Story with New Insight into How the Activity of Pd is influenced by Au. *Environ. Sci. Technol.* **2018**, *52*, 4244-4255.

(89) Jover, J.; Ratés, M. G.; López, N. The Interplay between Homogeneous and Heterogeneous Phases of PdAu Catalysts for the Oxidation of Alcohols. *ACS Catal*. **2016**, *6*, 4135−4143.

(90) Ureta-Zañartu, M. S.; Berríos, C.; González, T.; Fernández, F.; Báez, D.; Salazar, R.; Gutiérrez, C. Electrocatalytic Oxidation of Alcohols at Gold electrodes in Alkaline Media. *Int. J. Electrochem. Sci.* **2012**, *7*, 8905–8928.

(91) Zeis, R.; Lei, T.; Sieradzki, K.; Snyder, J.; Erlebacher, J. Catalytic Reduction of Oxygen and Hydrogen Peroxide by Nanoporous Gold. *J. Catal*. **2008**, *253*, 132−138.

(92) Jirkovsky, J. S.; Panas, I.; Ahlberg, E.; Halasa, M.; Romani, S.; Schiffrin, D. Single Atom Hot-Spots at AuPd Nanoalloys for Electrocatalytic H_2O_2 Production. *J. Am. Chem. Soc.* **2011**, *133*, 19432−19441.

(93) Cherevko, S.; Topalov, A. A.; Zeradjanin, A. R.; Katsounaros, I.; Mayrhofer, K. J. Gold Dissolution: Towards Understanding of Noble Metal Corrosion. *RSC Adv*. **2013**, *3*, 16516–16527.

(94) Durovic, M. D.; Puchta, R.; Bugarcic, Z. D.; van Eldik, R. Studies on the Reactions of $[AuCl_4]^-$ with Different Nucleophiles in Aqueous Solution. *Dalton Trans*. **2014**, *43*, 8620−8632.

(95) Feng, J.; Ma, C.; Miedziak, P. J.; Edwards, J. K.; Brett, G. L.; Li, D.; Du, Y.; Morgan, D. J.; Hutchings, G. J. Au−Pd Nanoalloys Supported on Mg-Al Mixed Metal Oxides as a

Multifunctional Catalyst for Solvent-Free Oxidation of Benzyl Alcohol. *Dalton Trans.* **2013**, *42*, 14498−14508.

(96) Fang, W. H.; Chen, J. S.; Zhang, Q. H.; Deng, W. P.; Wang, Y. Hydrotalcite-Supported Gold Catalyst for the Oxidant-Free Dehydrogenation of Benzyl Alcohol Studies on Support and Gold Size Effects. *Chem-Eur. J.* **2011**, *17*, 1247−1256.

TOC

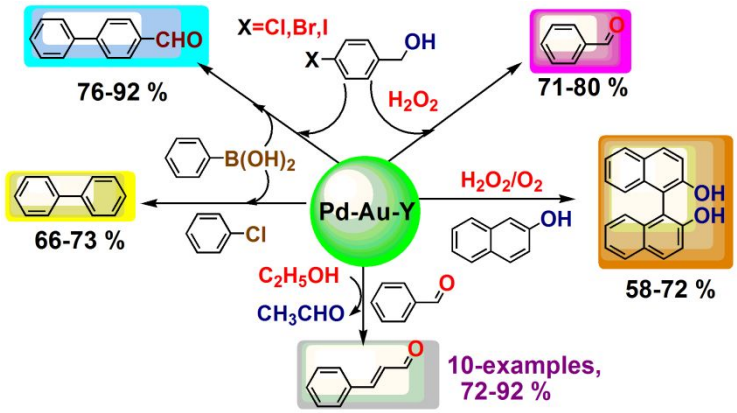

Pd-Au-Y as active catalyst for boosting single and multicomponent reaction